Rheology of liquid foam

2005 J. Phys.: Condens. Matter 17 R1041

(http://iopscience.iop.org/0953-8984/17/41/R01)

INSTITUTE OF PHYSICS PUBLISHING JOURNAL OF PHYSICS: CONDENSED MATTER

J. Phys.: Condens. Matter **17** (2005) R1041–R1069 doi:10.1088/0953-8984/17/41/R01

TOPICAL REVIEW

Rheology of liquid foam

R Höhler and S Cohen-Addad

Laboratoire de Physique des Matériaux Divisés et des Interfaces, Université de Marne-la-Vallée, UMR 8108 du CNRS, 5 Boulevard Descartes, 77 454 Marne-la-Vallée cedex 2, France

Received 14 June 2005, in final form 4 August 2005
Published 30 September 2005
Online at stacks.iop.org/JPhysCM/17/R1041

Abstract

Liquid foams can behave like solids or liquids, depending on the applied stress and on the experimental timescale. Understanding the origin of this complex rheology which gives rise to many applications and which resembles that of many other forms of soft condensed matter made of closely packed soft units requires challenging theoretical questions to be solved. We briefly recall the basic physics and physicochemistry of foams and review the experiments, numerical simulations and theoretical models concerning foam rheology published in recent years.

(Some figures in this article are in colour only in the electronic version)

Contents

0953-8984/05/411041+29$30.00

1. Why study foam rheology?

Liquid foams are concentrated dispersions of gas bubbles in a surfactant solution. Although they are constituted only of fluids, their mechanical properties can be either solid-like or liquid-like (Weaire and Hutzler 1999), depending on the applied stress, as illustrated in figure 1. The elasticity of liquid foams arises because a small applied stress increases the gas–liquid interfacial area and thus the energy per unit volume, as shown by Derjaguin and later by Princen in their pioneering work (Derjaguin 1933, Princen and Kiss 1986). If the applied stress is increased beyond the yield stress, it triggers irreversible bubble rearrangements and foam flows like a viscous non-Newtonian fluid.

The uncommon mechanical behaviour of foams combined with their low density and their large specific surface area give rise to a large variety of industrial applications (Khan and Prud'homme 1996). For instance, in the widely used process called flotation, liquid foams are employed to separate minerals from extracted ore. Foams are used as drilling fluids in oil production, and as fire fighting agents for polar solvent and oil fires. They are also valued as a galenic form of medical drugs that can enhance efficiency. In everyday life, they are encountered in many food products and cosmetics. In all of these applications, the foam rheology must be tuned to meet the requirements of the products or processes. To achieve this aim, a fundamental understanding of the underlying physics and physical chemistry is necessary.

Foams present characteristic structures on length scales ranging from macroscopic to molecular. We will show in this review that physical models of foam rheology can involve interplay between processes at all of these length scales. The difficulty of formulating such models raises the question of the level of coarse-graining necessary to allow maximum physical insight with minimal complexity. Schematically, foams may be described as disordered and metastable packings of small soft units. In this respect, they resemble other complex fluids such as concentrated emulsions (often called biliquid foams), soft pastes, particulate gels and even lyotropic multilamellar vesicles. All of these fluids present slow mechanical relaxations reminiscent of the behaviour of glassy materials, jamming and yielding at the crossover between solid-like and liquid-like behaviours, and coupling between ageing and dynamics. Therefore, the question arises of whether some aspects of this behaviour may be due to generic mechanisms acting on a mesoscopic length scale where the details of the physicochemical constitution do not matter. It has been conjectured that such mechanisms may govern a whole class of 'soft glassy materials' (Cates 2002, Sollich *et al* 1997). The differences between the intrinsic dynamics at the bubble, droplet or particle scale set a limit of such a 'universal' approach. In contrast to some emulsions and colloidal suspensions, the typical bubble radius in foams is far too large for thermal dynamics to be relevant. Nevertheless, foams do have an intrinsic source of dynamics since their structure evolves with time due to the effects of liquid drainage, bubble coalescence and interbubble gas diffusion. More detailed models of foam rheology describe bubbles as interacting spheres with elastic repulsion and viscous friction between first neighbours (Durian 1995, 1997). In this framework, sheared foam could be reminiscent of a supercooled liquid (Langer and Liu 2000). Finally, the equilibrium structure of foam minimizes the interfacial area for given bubble volumes. This simple and powerful principle allows very accurate simulations of quasistatic foam rheology, providing the link between behaviours at the macroscopic and the gas–liquid interface scales (Reinelt and Kraynik 2000, Weaire and Hutzler 1999).

The origin of the rheological behaviour of foam has been the subject of many recent experiments, numerical simulations as well as theoretical studies, and an understanding of the local physicochemical processes and properties that govern the macroscopic rheology is

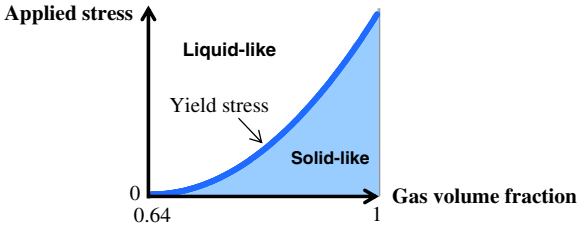

Figure 1. Schematic diagram of the solid-like and liquid-like behaviours of aqueous foams.

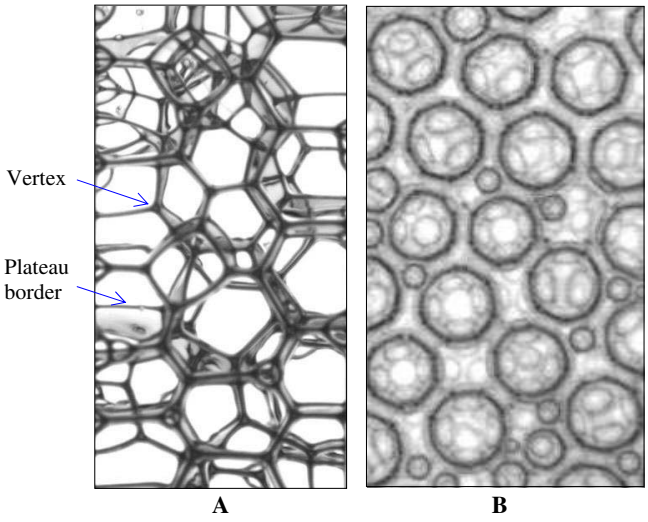

Figure 2. Typical structures of dry foam (A) and wet foam (B).

beginning to emerge. In the present topical review, we first recall basic concepts concerning foam structure, ageing and rheology. We then focus on linear and non-linear viscoelasticity and its interplay with ageing. Finally, yielding and liquid-like response are discussed.

2. Basic concepts, models and methods

2.1. Structure and ageing

On the macroscopic scale, foams appear to be homogeneous and may be characterized by their gas volume fraction, denoted as ϕ. A closer look reveals a packing of bubbles whose size is typically in the range 10 μm–1 cm. The thickness of the liquid films separating neighbouring bubbles is generally between 10 nm and a few μm. To prevent film rupture, the gas–liquid interfaces must be covered by surfactant molecules. In equilibrium, the pressure in the liquid is determined by the laws of hydrostatics, and the gas pressures in the bubbles differ from this due to capillary and disjoining pressures. Capillary pressure is by definition the difference in pressure between two contiguous gas and liquid phases, due to surface tension (Levich 1962). As described by Laplace's law, it varies linearly with the surface tension and mean interfacial curvature (Adamson 1990). Disjoining pressure in thin films results from intermolecular interactions, whose range does not exceed about 10^2 nm: van der Waals forces, electrostatic repulsions arising from the electrical double layers at the interfaces and steric interactions. Let us first consider foams whose liquid content is sufficiently small for the bubbles to have an approximately polyhedral shape as illustrated in figure 2(A). The bubble edges in such dry foams are called Plateau borders; the junctions of Plateau borders constitute vertices.

The structures of real foams are generally disordered, but not totally random: Plateau's rules state that for 3D foams in the dry limit and under equilibrium conditions three films must join at each Plateau border at mutual angles of 120°, and four Plateau borders must form tetrahedral symmetric vertices (Weaire and Hutzler 1999). Edges and vertices of valence higher than those given by these rules are mechanically unstable and dissociate into stable ones[1]. The topological statistics of dry random foams and their geometric properties related to surface area, edge length and stress have been evaluated by extensive computer simulations (Kraynik *et al* 2003, 2004). If more and more liquid is added to a dry 3D foam, the bubble shapes become approximately spherical (cf figure 2(B)). Such wet foams can have gas volume fractions down to a characteristic value close to 64% where their structure resembles a random close packing of spheres. At even lower gas volume fractions, foam loses its rigidity and behaves as a bubbly liquid.

Foams are intrinsically unstable and their structure evolves with time due to drainage, film rupture and gas diffusion across the films separating neighbouring bubbles. On a local scale, drainage corresponds to the liquid flow through films, Plateau borders and vertices. The first of these contributions consists in a thinning of the films driven by gravity and capillary suction and limited by the disjoining pressure (Bhakta and Ruckenstein 1997). The latter two contributions have been described theoretically by effective medium models where the liquid is assumed to flow as in a porous medium with the Plateau borders behaving as deformable pores (Verbist *et al* 1996, Neethling *et al* 2002, Saint-Jalmes *et al* 2000). This flow is driven by gravity and capillary forces, due to the curvature of the Plateau border interfaces, and it stops when the gradient of the capillary pressure balances gravity (Weaire and Hutzler 1999). To provide an accurate description, the viscous dissipation in both the Plateau borders and the vertices has been taken into account (Durand and Langevin 2002, Koehler *et al* 2000). Moreover, the flow boundary conditions at the gas–liquid interfaces, which depend on the surfactants used, need to be considered (Langevin 2000). A detailed discussion of this very active field of research is beyond the scope of the present review. Ultimately, when films become very thin, they rupture, leading to bubble coalescence. This process is strongly coupled to drainage (Bhakta and Ruckenstein 1997), and arises when the gas volume fraction increases above a threshold value depending on the surfactant and its concentration (Carrier and Colin 2003). It has been studied in a series of acoustic or conductivity experiments (Müller and Di Meglio 1999, Vandewalle and Lentz 2001, Carrier and Colin 2003).

Laplace pressure differences between neighbouring bubbles drive gas diffusion through the liquid films, so that larger bubbles grow at the expense of smaller ones: the foam coarsens. This leads to a build-up of local strain modifying the length of the bubble edges. When an edge length goes to zero, an unstable configuration is obtained and neighbour switching occurs. Such elementary topological changes, called T1 processes and illustrated in figure 3, can occur independently or as avalanches (Weaire and Hutzler 1999). They not only occur as a result of coarsening, but may also be induced by applying macroscopic strain. Individual T1 bubble rearrangements correspond in 2D to the dissociation of a fourfold vertex into two stable threefold vertices. T1 processes in 3D are more complex; a discussion can be found in the literature (Weaire and Fortes 1994, Reinelt and Kraynik 2000). A bubble vanishes when all of its gas has been transferred to its neighbours. Such topological changes are called T2 processes (cf figure 3). In the absence of significant drainage and coalescence, coarsening leads asymptotically to a scaling state where the bubble growth is statistically self-similar: the distribution of bubble sizes, normalized by their average value, becomes independent of time

[1] For foams of finite liquid content, it has been predicted that eightfold vertices can be metastable (Weaire and Phelan 1996).

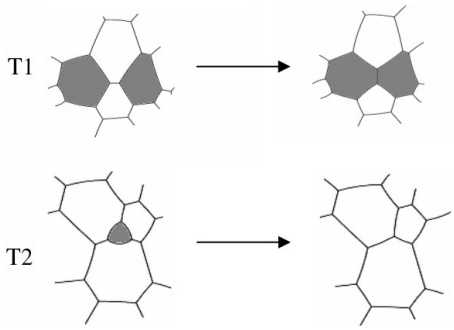

Figure 3. Illustration of T1 and T2 processes in dry 2D foam. Two bubbles that are initially separate and that become neighbours as a consequence of the T1 event are marked in grey. The same shade is used to distinguish a bubble that disappears upon a T2 event.

as well as initial conditions. A mean field argument based on statistical self-similarity predicts for 3D as well as 2D foams that the average bubble radius, denoted as R_1, increases with age t following a parabolic law (Mullins 1986):

$$R_1^2(t) - R_1^2(t_0) = K(t - t_0). \tag{1}$$

The constant K has the dimension of a diffusion coefficient and depends on the permeability of the individual liquid films, governed by their thickness as well as the solubility and the diffusion coefficient of the gas in the liquid (Princen and Mason 1965). Moreover, it has been shown that K is an increasing function of gas volume fraction (Vera and Durian 2002). The bubble growth law equation (1) has been verified experimentally in 2D (Glazier and Weaire 1992) and in 3D (Durian *et al* 1991, Hoballah *et al* 1997). As a consequence of statistical self-similarity, there is only one independent characteristic length scale describing the foam structure, which can be chosen as R_1. The temporal evolution of any mth moment of the bubble radius distribution, denoted as $R_m(t)$, is therefore proportional to that of R_1 taken to the mth power (Hoballah *et al* 1997). Depending on their characteristic timescales, drainage and coarsening may be coupled and mutually accelerate (Hilgenfeldt *et al* 2001a, Hutzler and Weaire 2000, Saint-Jalmes and Langevin 2002, Vera and Durian 2002). Note that drainage, coalescence and coarsening also exist in emulsions, but since the preponderant process is determined by the differences in density and solubility between the dispersed and continuous phases, the ageing dynamics of foams and emulsions can differ significantly.

2.2. Rheology

Measures of stress and strain. On a macroscopic scale, foam may be viewed as a continuum, and the stress tensor is a well defined quantity. However, the continuum picture breaks down on the bubble scale. In steadily flowing foam, a local stress can be obtained by performing a temporal average over the pressure and interfacial tension forces acting on a surface element (or a line element in 2D foam) of fixed position (Asipauskas *et al* 2003). A general expression for the local interfacial and gas pressure contributions to the macroscopic stress σ has been proposed by Bachelor (1970):

$$\sigma_{ij} = -\frac{1}{NV}\sum_{k=1}^{N}(p_k V_k)\delta_{ij} + \frac{T}{NV}\int\int(\delta_{ij} - n_i n_j)\,\mathrm{d}S \tag{2}$$

p_k and V_k are respectively the gas pressure and volume of bubble number k, N is the total number of bubbles, V is the average bubble volume, T the interfacial tension and $\mathbf{n}$ a unit vector normal to the interface. The integration is carried out over all interfaces in the volume. Both faces of each soap film have to be taken into account. Equation (2) is extensively used in numerical simulations and analytical models.

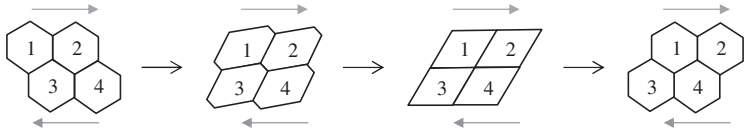

Figure 4. 2D foam structures obtained by applying an increasing shear strain as indicated. A T1 process occurs as bubbles marked 2 and 3 separate and the topology changes.

Strain can be defined on the macroscopic scale by comparing the previous and present positions of each volume element, denoted as $\mathbf{x}'$ and $\mathbf{x}$ respectively. Only if very small strains and linear rheology are considered is the infinitesimal strain tensor ε adequate for describing the deformation. To study non-linear effects, the deformation gradient tensor $\mathbf{F}$, the Finger strain tensor $\mathbf{B}$ or the right Cauchy–Green tensor $\mathbf{C}$ must be used (Macosko 1994, Mal and Singh 1991):

$$\mathbf{F} = \frac{\partial \mathbf{x}}{\partial \mathbf{x}'}; \qquad \mathbf{B} = \mathbf{F}\mathbf{F}^{\mathbf{T}}; \qquad \mathbf{C} = \mathbf{F}^{\mathbf{T}}\mathbf{F}; \qquad \varepsilon = \tfrac{1}{2}(\mathbf{F} + \mathbf{F}^{\mathbf{T}}) - \mathbf{I}. \tag{3}$$

$\mathbf{I}$ is the unit tensor. As in the case of stress, a continuous tensor field is inadequate for describing strain on the bubble scale: even if the macroscopic strain is homogeneous, the deformation of individual bubbles is generally non-affine, corresponding to a deformation gradient which varies strongly over small distances. The local deformation in foam may be described statistically by viewing the interfaces as an ensemble of small flat elements, characterized by their area and a normal vector $\mathbf{n}$ (Doi and Ohta 1991). A distribution function $f(\mathbf{n})$ is introduced such that the area of surface elements per unit volume whose normal lies within a solid angle $\mathrm{d}\Omega$ around $\mathbf{n}$ is $f(\mathbf{n})\,\mathrm{d}\Omega$. This description of strain is used in the models of non-linear foam rheology presented in section 3.2. Moreover, the statistical properties of the distribution $f(\mathbf{n})$ have recently been discussed in relation to equation (2) (Fortes *et al* 2002). As an alternative statistical measure of strain in dry foams, a texture tensor $\mathbf{M} = \langle \ell \otimes \ell \rangle$ has been proposed, where ℓ is a vector going from one vertex to a neighbouring vertex and the angular brackets represent an average over a region in the foam. From $\mathbf{M}$, a 'statistical strain tensor' has been derived which reduces for small deformations to the average infinitesimal strain tensor (Aubouy *et al* 2003).

Basic rheology of ordered foams. Even though perfect bubble 'crystals' are rare in nature, such systems are useful for studying theoretically basic mechanisms of foam rheology on the bubble scale. Pioneering work in this field was focused on dry 2D foam whose bubbles are hexagonal in the absence of stress (Khan and Armstrong 1986, Princen 1983). When such foam is subjected to a small quasistatic shear strain, vertices move in a non-affine way since Plateau's rules must be respected (cf figure 4). The total edge length per unit cell which determines the elastic energy density increases to a good approximation quadratically with strain, corresponding to linear elastic response.

A critical configuration is reached at the yield strain $2/\sqrt{3}$ where the length of the edge separating bubbles marked 2 and 3 in figure 4 shrinks to zero (Princen 1983). Further increase of strain induces a topological rearrangement, called a T1 process (cf section 2.1). From here on, foam will not return elastically to its initial configuration if stress is relaxed to zero, but it will settle into a new equilibrium, corresponding to a structure with permanent plastic strain. The yield stress is defined as the stress required to induce such rearrangements, corresponding to the onset of liquid-like rather than elastic response (Larson 1999). Extensive studies of the

rheology of polydispersed ordered 2D foams as well as of 3D ordered foams can be found in the literature (Kraynik and Reinelt 1996, Reinelt and Kraynik 1993, 2000).

Mesoscopic models. Disordered packings of small soft units, such as foams, concentrated emulsions and soft pastes show strikingly similar rheological behaviour. This observation has prompted several authors to conjecture that the macroscopic response can be explained in terms of generic physical mechanisms. For a recent review, see Barrat *et al* (2003). One approach consists in considering the material on a mesoscopic length scale, large enough for continuum mechanics concepts such as stress, strain and yield strain to be well defined and small enough that spatial variations of these quantities can be resolved. In the soft glassy rheology models, all mesoscopic regions are supposed to present a linear elastic response up to a maximum local elastic energy E, randomly chosen from a distribution $\rho(E)$ (Sollich 1998, Sollich *et al* 1997). The macroscopic stress is taken to be the average of the mesoscopic stresses and the time evolution of each mesoscopic strain follows the evolution of the imposed macroscopic strain as long as there are no rearrangements. If the local elastic energy exceeds E, a structural rearrangement occurs, all the elastic energy is dissipated and a new value of E is chosen. Rearrangements may also be activated by strain fluctuations, represented in a mean field approach by an effective noise temperature ζ. It has been shown that the choice $\rho(E) \propto \exp[-E/\zeta]$ with a specific value for ζ leads to a rheological constitutive equation that qualitatively describes many features of the behaviour observed for soft pastes, emulsions and foams. This form of $\rho(E)$ had previously been proposed to describe glassy behaviour (Bouchaud 1992). Another group of models are based on a scalar measure of the 'degree of jamming', determined by two opposing tendencies: local flow breaks up the jammed structure, speeds up the dynamics and reduces the viscosity. Conversely, ageing re-establishes the jammed structure and thereby enhances the viscosity. This is expressed in terms of non-linear differential equations that reproduce at least qualitatively much of the experimentally observed phenomenology (Coussot *et al* 2002a, Derec *et al* 2001, Picard *et al* 2002). Let us finally note that a mode coupling approach has also been used to derive a generic model of complex yield stress fluids (Hébraud and Lequeux 1998). Even though foams and emulsions are often cited as possible examples of real materials described by the models outlined here, the link with the known physics at the bubble or droplet scale has not yet been established.

Numerical simulation techniques. Four principal techniques have been used to simulate foam rheology and ageing. The first is based on the principle that in static equilibrium, foam has a structure of minimal interfacial energy and thus minimal interfacial area. The Surface Evolver software allows one to determine the structure of minimal energy numerically, for given boundary conditions, such as walls confining the foam (Brakke 1992). Each interface is discretized into finite elements and this meshing is refined according to the required accuracy. By applying step by step small changes of the boundary conditions, quasistatic experiments such as shearing ones can be simulated, as illustrated in figure 5. For isochoric macroscopic strains, the volume of each bubble is kept constant upon minimization since the capillary pressure is generally many orders of magnitude too small to compress the gas significantly. The principal strength of Surface Evolver simulations is their accuracy; their main shortcomings are the restriction to the quasistatic regime and the very large amount of computer memory and time required to simulate large structures, especially in 3D.

The following three models resolve these two difficulties by means of simplified descriptions of foam structure, dynamics and dissipation. The gain of computational efficiency is obtained at the expense of realism and possible artefacts that need to be checked for. In the vertex model, the foam structure is described only in terms of the positions of the vertices.

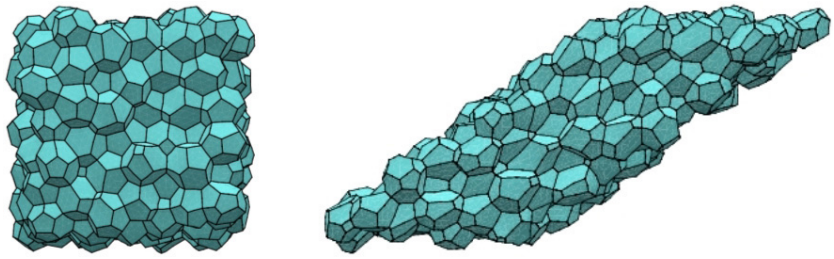

Figure 5. Two samples of dry random monodisperse 3D foam, obtained by a Surface Evolver simulation with periodic boundary conditions. The structure on the left is not strained whereas the one on the right is subjected to a simple shear of magnitude 1.4. (Figure provided by A Kraynik.)

In this framework, foam dynamics is described by approximate equations of motion for the vertices, taking into account dissipation in the liquid films (Okuzono *et al* 1993). The Potts model was first used to study coarsening of grains in polycrystals (Grest *et al* 1988) and then that of bubbles in aqueous foams (Glazier *et al* 1990). It uses a discrete space in which spin-like variables distinguish the regions of the sample occupied by each grain or bubble. Simple spin dynamics allows coarsening to be simulated. This simulation technique was later refined to describe shearing and viscous dissipation (Jiang *et al* 1999). In the 'bubble model', the foam structure is described by the central position and radius of each bubble (Durian 1995, 1997). Dissipation has been described in this framework either as a friction between neighbouring bubbles proportional to their relative speed or, in a mean field approach, as a friction proportional to the bubble speed relative to the average speed of the neighbours. Moreover, neighbouring bubbles interact via a repulsive harmonic potential if the distance between their centres is smaller than the sum of their respective radii. Numerical simulations using the Surface Evolver as well as analytical arguments have shown that in 2D, elastic interactions between bubbles can indeed be described to a good approximation by a pairwise harmonic potential whose range is set by the sum of the bubble radii (Lacasse *et al* 1996). However, in 3D, the interaction is anharmonic and non-local: its characteristics depend on the number of neighbours in contact with the interacting pair of bubbles (Lacasse *et al* 1996, Morse and Witten 1993). On the basis of interaction potentials taking into account these effects, 3D bubble model simulations of flowing foams have been carried out (Gardiner *et al* 2000).

Experimental techniques. Foams can be studied using the standard methods of rheometry (Macosko 1994), but several specific points have to be kept in mind. Wall slip may occur at the contact of the foam and the surfaces of the cylinders, cones or plates of the rheometer. The study of bubbles slipping on a wetted solid surface goes back to the work of Bretherton (1961), but extending these results to wall slip of 2D or 3D foams requires a more specific analysis (Cantat *et al* 2004, Denkov *et al* 2005). Various procedures in rheometry have been proposed to correct for wall slip, in particular in the context of pipe viscosimetry (Calvert 1990, Enzendorfer *et al* 1995, Gardiner *et al* 1998a, Herzhaft *et al* 2005), a vast subject which we will not discuss in detail here. In most recent rheological studies using cone–plate, plate–plate or Couette rheometers, wall slip has been eliminated by roughening the surfaces in contact with the sample. Another intrinsic difficulty of foam rheometry is that the sample structure continuously evolves due to the mechanisms reviewed in section 2.1. Slow rheological response is therefore intrinsically coupled to ageing. This may explain why most reported measurements focus on very stable foams.

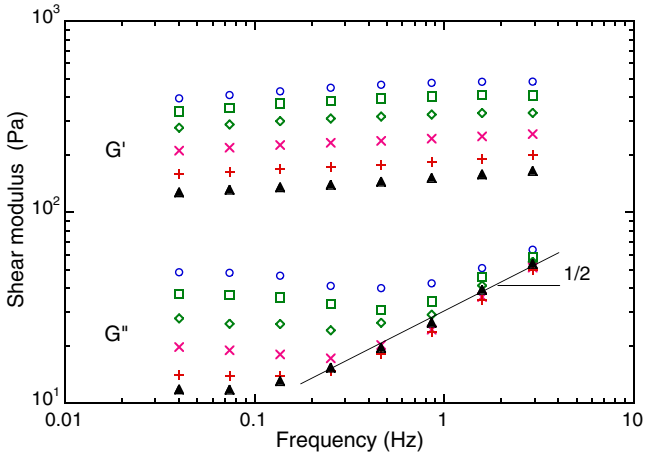

Figure 6. Storage and loss moduli G' and G'' of Gillette shaving cream ($\phi = 92.6\%$) plotted versus frequency. These samples that evolve on the experimental timescale only due to coarsening are subjected to a sinusoidal shear stress of amplitude much smaller than the yield stress. The symbols correspond to different foam ages: (○) 15 min, (□) 30 min, (◇) 1 h, (×) 2 h, (+) 4 h, (▲) 8 h. (Reprinted figure, with permission from Cohen-Addad *et al* (1998), Copyright 1998 by the American Physical Society.)

3. Solid-like response

3.1. Linear viscoelasticity

Comparison with other complex fluids and the existence of a linear viscoelastic regime. The linear viscoelastic response observed for foams is in many respects similar to that of other disordered close packings of small soft units, such as concentrated emulsions and soft pastes. The complex shear modulus $G^*(\omega) = G'(\omega) + \mathrm{i}G''(\omega)$ behaves in a regime of high angular frequency ω as if a viscoelastic contribution proportional to $(\mathrm{i}\omega)^{1/2}$ were superposed on a constant purely elastic shear modulus. Indeed, G'' presents an increase with frequency proportional to $\omega^{1/2}$ that can be clearly distinguished at frequencies typically above 1–10 Hz. The increase of G' with frequency becomes significant compared to the static elasticity only at much higher frequencies. This behaviour is observed for concentrated emulsions (Hébraud *et al* 2000, Liu *et al* 1996), wet foams (Cohen-Addad *et al* 1998, Gopal and Durian 2003) and pastes (Derec *et al* 2003). At low frequency, an extended plateau of $G'(\omega)$ has been observed in all of the above-mentioned materials. $G''(\omega)$ also presents a plateau, but its extent as well as the ratio G'/G'' depend on physicochemical properties (Labiausse 2004) and foam age (Cohen-Addad *et al* 1998), as illustrated in figure 6. It has been pointed out that even minute strains might trigger irreversible structural changes in foams which would be incompatible with a strictly linear response (Weaire and Fortes 1994). However, in oscillatory experiments, the observed dependence of G' and G'' on the strain amplitude for small amplitudes is weak, suggesting a linear response. Furthermore, the sample volume fraction where bubble motion is strictly periodic in sinusoidally sheared foam has been monitored using diffusing-wave spectroscopy echoes (Höhler *et al* 1997), an optical technique based on multiple scattering of coherent light. In the range of strain amplitudes where the measured rheological response is linear, no strain induced bubble rearrangements were detected (Höhler *et al* 1997, Labiausse 2004). Finally, if the viscoelastic response is linear, the frequency dependent complex shear modulus must be related via a Fourier transform to the stress response measured as a function

of time after the application of a step strain (Ferry 1980). This prediction has been confirmed experimentally for wet foams (Gopal and Durian 2003). These observations clearly establish the existence of a well defined linear viscoelastic regime.

Linear elasticity. When a small constant macroscopic shear stress is applied to a foam sample, the bubbles are deformed and thus their surface area and interfacial energy increase, giving rise to an elastic strain. Under static conditions, this linear elastic behaviour is described by an elastic shear modulus denoted as G_0, corresponding approximately to the plateau of $G'(\omega)$ shown in figure 6. In early experiments on emulsions, G_0 was found to be proportional to the interfacial tension T and to the inverse of the Sauter mean bubble radius $R_{32} \equiv R_3/R_2$ which is a measure of the amount of interfacial area per unit volume (Princen and Kiss 1986). In numerical simulations of 3D dry random monodispersed and polydispersed foam, $G_0 = 0.51T/R_{32}$ has been obtained (Kraynik and Reinelt 2004, Kraynik *et al* 2000), in agreement with an approximate theoretical prediction (Stamenovic 1991). These results are consistent with previously computed shear moduli of ordered 3D dry foams if isotropic averaging is applied (Kraynik and Reinelt 1996, Reinelt and Kraynik 2000). Quantitative comparison with experimental data is non-trivial, since in response to a step stress, real foams slowly creep and do not settle into a truly static equilibrium, as will be explained below. Another difficulty is the experimental determination of the bubble size distributions in foams. It is generally estimated from observations of the sample surface, making it hard to determine bulk averages such as R_1 or R_{32} accurately. Moreover, many authors only report the mean radius R_1 which is only in the case of monodispersed samples equal to the Sauter mean radius, needed for a quantitative discussion of elasticity. Finally, extrapolation of the shear modulus to the dry limit is non-trivial: a recent theoretical analysis of very dry foam predicts a contribution to the shear modulus, scaling as the square root of the liquid fraction (Kern and Weaire 2003). With these words of caution in mind, we note that a linear extrapolation to the dry limit of the data shown in figure 7 for monodispersed emulsions (Mason *et al* 1995) and polydispersed emulsions (Princen and Kiss 1986) at low frequencies or long experimental timescales agrees approximately with the prediction $G_0 = 0.5T/R_{32}$. Moreover, experiments using foams (Saint-Jalmes and Durian 1999) and emulsions (Mason *et al* 1995) with a wide range of volume fractions of the dispersed phase have shown that the elasticity vanishes at $\phi = \phi_c \cong 0.64$, close to the fraction of random close packing of monodisperse hard spheres. This loss of rigidity at $\phi = \phi_c$ has been described theoretically as a percolation phenomenon (Bolton and Weaire 1990). For $\phi_c < \phi < 1$, G_0 obtained from G' measurements at low frequencies has been found to vary as $\phi(\phi - \phi_c)$ in emulsions (Mason *et al* 1995) and foams (Saint-Jalmes and Durian 1999). Mason, Bibette *et al* have proposed to describe the monodisperse emulsion data with the following empirical relation (Mason *et al* 1995) and a dimensionless prefactor $\alpha \cong 1.6$:

$$G_0 = \alpha\phi(\phi - \phi_c)\frac{T}{R_1}. \tag{4}$$

Note that values of α lower than 1.6 were found in several measurements with polydisperse foams as shown in figure 7. Moreover, equation (4) is consistent with numerical simulations for polydispersed dry foam cited above if R_1 is replaced by R_{32} and $\alpha \cong 1.4$. Additional accurate experimental work and a better understanding of viscoelastic effects would be of great interest for making further progress.

Origin of the slow linear viscoelastic response. On the basis of early 2D quasistatic numerical simulations as well as 3D relaxation modulus measurements, it has been suggested that the

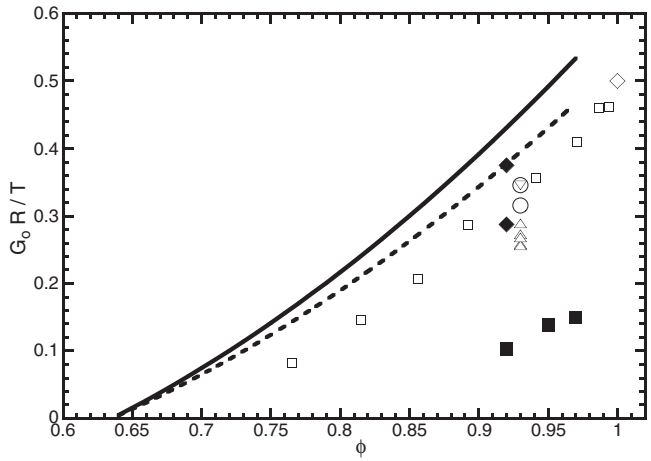

Figure 7. Static shear modulus G_0, normalized by the surface tension T divided by a mean bubble radius R, versus volume fraction of the dispersed phase ϕ, for foams and oil in water emulsions of different polydispersity. For emulsions, ϕ represents the effective volume fraction taking into account the thickness of the thin water film due to the screened Coulomb repulsion between the droplets. Open symbols represent data where $R = R_{32}$ whereas for lines and full symbols $R = R_1$: (——) fit to monodisperse emulsion data using equation (4) with $\alpha = 1.6$ (Mason *et al* 1995); (– – –) fit to polydisperse foam data using equation (4) with $\alpha = 1.4$ (Saint-Jalmes and Durian 1999); (□) polydisperse emulsion (Princen and Kiss 1986); (■) polydisperse foam (Khan *et al* 1988); (⧫) Gillette foam (Gopal and Durian 1999, 2003); (▽, ○) polydisperse foams and (△) Gillette foam (Cohen-Addad and Höhler 2004); (◇) Surface Evolver simulation of polydisperse foams (Kraynik and Reinelt 2004).

slow viscoelastic relaxation of foams may be governed by the coarsening process (Weaire and Kermode 1984, Gopal and Durian 2003). To gain more insight, the long time end of the linear viscoelastic relaxation spectrum has been probed by means of creep experiments (Cohen-Addad *et al* 2004): a stress step much smaller than the yield stress is applied to the sample and the resulting strain is measured as a function of time. Such data obtained for wet foams show an initial elastic response, followed by a transient relaxation lasting a few seconds and finally a steady state flow where strain increases linearly with time (cf figure 8). The measured creep compliance $J(t)$, defined as the strain $\gamma(t)$ at time t divided by the fixed amount of applied stress σ_{12}, is well described by an expression of the form Cohen-Addad *et al* (2004):

$$J(t) \equiv \frac{\gamma(t)}{\sigma_{12}} = J_0 + \frac{t}{\eta_0} + J_1(1 - \exp(-t/(J_1\eta_1))) \tag{5}$$

where the parameters J_0, J_1, η_0 and η_1 depend on the physicochemical characteristics of the foam. Note that $J_0 = 1/G_0$. Recent creep experiments on other kinds of surfactant and protein foams are in full agreement with equation (5) (Marze *et al* 2005). Thus, in contrast to the large spectrum of relaxation times predicted by the soft glassy rheology models (cf section 2.2), the slow relaxations in the foams studied are due to only two processes: steady creep governed by the characteristic time $\eta_0(J_0 + J_1)$ and a transient relaxation on the timescale $\eta_1 J_1$. The link between creep and coarsening has been clarified by rheological measurements coupled *in situ* to diffusing-wave spectroscopy investigations of the local bubble dynamics. On the basis of such data, creep has been explained as a consequence of intermittent local loss of elasticity upon coarsening induced structural rearrangements on the bubble scale (Cohen-Addad *et al* 2004). This mechanism has been described by a mesoscopic model relating the characteristic

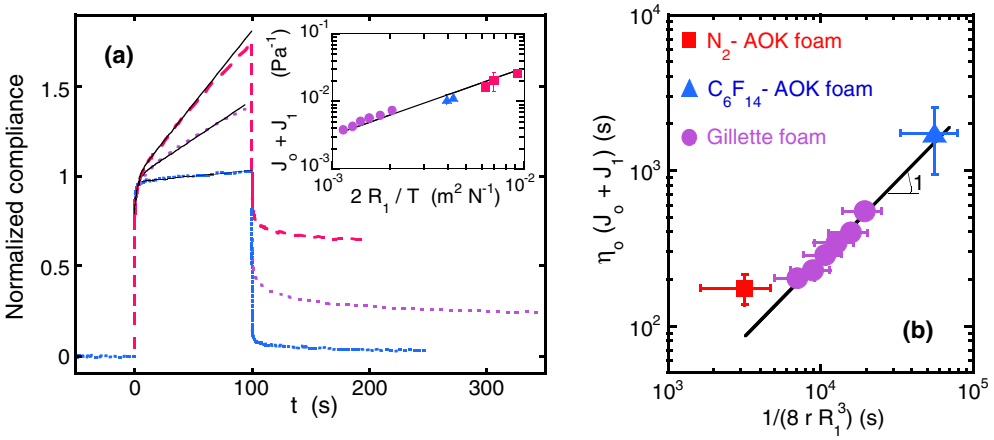

Figure 8. (a) Typical shear creep and recovery compliances as a function of time, measured for a stress applied for 100 s starting at the instant $t = 0$. The applied stress is far below the yield stress and the compliances are normalized by the steady state compliance $J_0 + J_1$. The different line styles correspond to three kinds of foams: (- - - -) Gillette foam and two foams produced using an aqueous solution containing an α-olefine surfactant, polyethylene oxide, dodecanol and different gases: nitrogen for (– – –) N_2 foam and a mixture of nitrogen and perfluorohexane vapour for (· · · · · ·) N_2/C_6F_{14} foam. The inset shows $J_0 + J_1$ as a function of the average bubble diameter divided by surface tension T for the three kinds of foams, together with a linear fit: N_2 foam (■), Gillette foam (●) and N_2/C_6F_{14} foam (▲). (b) Characteristic time of the steady state creep, $\eta_0(J_0 + J_1)$, represented as a function of the average time interval between bubble rearrangements in a volume $(2R_1)^3$, for foams of widely differing coarsening rates. The line is a linear fit to the data on Gillette and N_2/C_6F_{14} foam with an average effective volume of a relaxed region $v_m = (6R_1)^3$. (Figures modified with permission from Cohen-Addad *et al* (2004), Copyright 2004 by the American Physical Society.)

time $\eta_0(J_0 + J_1)$ to r, the number of rearrangements per unit time and volume, and v_m, the effective average volume of the region where the local stress is relaxed upon a rearrangement: $\eta_0(J_0 + J_1) \cong (r v_m)^{-1}$. As shown in figure 8, this prediction is in good agreement with data for wet foams over a wide range of bubble rearrangement rates. v_m is found to be of the order of $(6R_1)^3$. The transient creep response is characterized by the compliance J_1 and viscosity η_1 which have been found experimentally to scale with bubble size as $J_1 \propto R_1$ and $\eta_1 \propto R_1^{-1.2}$. Among the many mechanisms of dissipation in foams discussed in the literature (Buzza *et al* 1995), dilatational surface friction at the gas–liquid interfaces is the only one compatible with this experimental evidence for η_1. It is predicted to give rise to an effective zero-shear foam viscosity of the order of κ/R_1 where κ is the dilatational surface viscosity. The elasticity described by the compliance J_1 can be associated with the following mode of structural relaxation: the abrupt bubble deformation upon the applied stress step is governed by viscous forces and therefore gives rise to a foam structure which is not of minimal interfacial energy. As time progresses, surface tension forces become dominant and the structure relaxes towards an equilibrium with minimal interfacial energy. A rough estimate of the characteristic time of this relaxation has been obtained from a 2D hexagonal foam model, using an approach similar to that of Kraynik and Hansen (1987) with a modified tensile force acting on a film of length L given by $2T + (2\kappa/L)(\partial L/\partial t)$ (Edwards *et al* 1991). The predicted relaxation time scales as κ/T with a prefactor of the order of 1. For this to be consistent with the experimentally measured value of the characteristic relaxation time $\eta_1 J_1$, κ must be of the order of 0.1 kg s^{-1} for the foaming solutions used in the experiments (Cohen-Addad *et al* 2004). This is in rough

agreement with dilatational surface viscosities reported for similar mixtures of sodium lauryl sulfate and dodecanol (Djabbarah and Wasan 1982).

To summarize, we note that the slow linear viscoelastic behaviour of wet foams strongly depends on the physicochemical properties of the liquid films. This response is described by equation (5) which may be represented by an association in series of a Maxwell element and a Voigt element. The former describes coarsening induced bubble rearrangements and the latter results from a structural relaxation mode, involving interfacial dilatational friction of the interfaces. Indeed, the dilatational viscous stress is not simply additive to elastic stress as pointed out previously (Hemar *et al* 1995).

Fast viscoelastic response. As mentioned in the introduction of this section, wet foams behave at sufficiently high frequencies as if a term proportional to $(\mathrm{i}\omega)^{1/2}$ were superposed on their low frequency complex shear modulus. As a possible origin of this fast viscoelastic response, one may consider the relaxation of individual bubbles, represented schematically as a spring whose modulus scales as T/R_1, and a dashpot describing dissipation mechanisms such as viscous shear flow of the liquid between bubbles (Buzza *et al* 1995, Hemar *et al* 1995). These hypotheses lead to a characteristic relaxation time $t_\mathrm{b} \propto \eta R_1^2/(Te)$ where e is the thickness of films (Durian 1995, 1997). For a wet foam, with $R_1 = 30\ \mu$m, $T = 30$ mN m^{-1}, $e = 1\ \mu$m and η equal to the viscosity of water, one obtains $t_\mathrm{b} \approx 10^{-5}$ s. Since this is orders of magnitude faster than the experimental timescale of typical rheological experiments, it has been suggested that collective rather than individual bubble relaxations could explain the viscoelastic response discussed above (Durian 1997). Liu *et al* have proposed that a disordered bubble or droplet packing may be described as an elastic matrix in which weak regions are randomly dispersed. In these regions, layers of bubbles may slip against each other along randomly oriented planes if the foam is subjected to a small strain (Liu *et al* 1996). Similar behaviour has indeed been observed in numerical simulations of disordered 2D foam (Langer and Liu 1997). The viscoelastic relaxation time in a weak region depends not only on the viscous drag of the sliding bubble layers and the elasticity of the surrounding foam but also on the orientation of the weak plane with respect to the applied shear. Random distribution of orientations leads to a distribution of relaxation times such that the experimentally observed scaling $G'' \propto \omega^{1/2}$ is obtained (Liu *et al* 1996). Let us note that processes at the scale of the gas–liquid interfaces may also contribute to the fast viscoelastic relaxations (Buzza *et al* 1995). Furthermore, in simulations of 2D foams confined between solid plates, a relatively fast relaxation related to viscous friction of bubbles on the walls has been evidenced (Cox 2005). It is superposed on a coarsening induced relaxation which is generally very slow, as discussed above.

Evolution of the viscoelastic behaviour upon coarsening. If drainage and coalescence are negligible on the experimental timescale, the coarsening process leads to a scaling state where the average bubble size $R_1(t)$ grows following a parabolic law (cf equation (1)). Experiments for wet foam have shown that the following empirical scaling law captures the evolution of the complex shear modulus under these conditions (Cohen-Addad *et al* 1998):

$$G^*(\omega, t) = b(t)G^*(\omega a(t), t_0). \tag{6}$$

The scaling factors $a(t)$ and $b(t)$ are by definition equal to one at the arbitrary reference time t_0. This law allows the data of figure 6 to be collapsed onto the two master curves shown in figure 9. To check the validity of equation (6) on very long timescales, the measured creep compliance $J(t)$ of wet foams described by equation (5) can be converted to complex shear modulus data at very low frequency using the relation $G^*(\omega) = 1/(\mathrm{i}\omega\mathcal{L}[J(t)][\mathrm{i}\omega])$ which is of general validity in linear viscoelasticity (Ferry 1980) and where $\mathcal{L}$ denotes the Laplace transform.

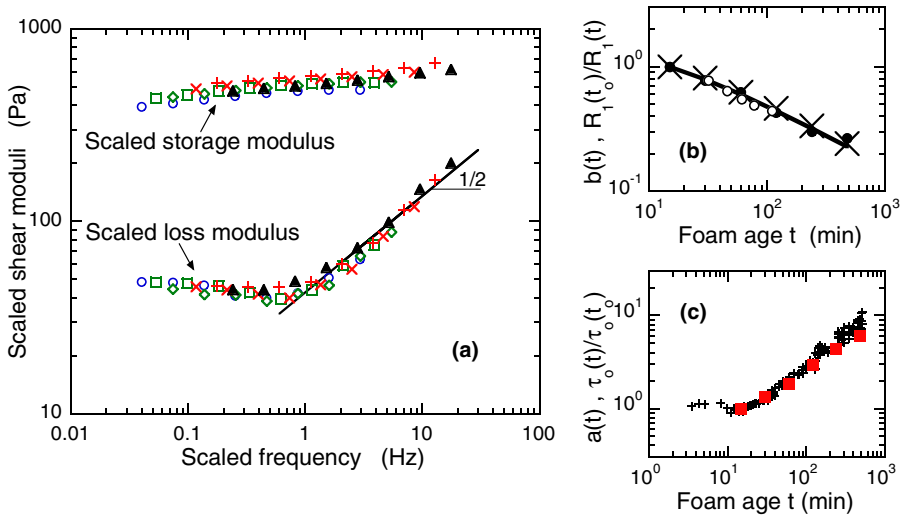

Figure 9. (a) Scaled shear moduli $G^*(\omega, t)/b(t)$ versus scaled frequency $\omega a(t)$, obtained from the data of figure 6 for different foam ages t. The straight line represents a power law of exponent 1/2, fitted to the data for scaled frequencies above 2 Hz. The age $t_0 = 15$ min is taken as a reference. (Reprinted figure, with permission from Cohen-Addad *et al* (1998), Copyright 1998 by the American Physical Society.) (b) Temporal evolution of the modulus scaling factor $b(t)$: (●) from oscillatory data (equation (6)), (○) from creep data (equation (7)), compared to (×) the temporal evolution of $1/R_1(t)$ (Cohen-Addad and Höhler 2004). The continuous line represents a fit of the inverse of a parabolic law (cf equation (1)) to the $b(t)$ data. (c) (■) Frequency scaling factor $a(t)$ and (+) average time interval between coarsening induced bubble rearrangements at a given place, denoted as $\tau 0(t)$, versus foam age. The latter data, measured by diffusing-wave spectroscopy, are normalized by their value at $t_0 = 15$ min (Cohen-Addad and Höhler 2001).

The expression obtained may be simplified by noting that $J_1 \ll J_0$ and by expanding G^* to first order in J_1/J_0:

$$G^*(\omega, t) \cong \frac{1}{J_0}\left(\frac{\mathrm{i}\omega\eta_0 J_0}{1+\mathrm{i}\omega\eta_0 J_0} - \frac{J_1}{J_0}\frac{(\omega\eta_0 J_0)^2}{(-\mathrm{i}+\omega\eta_0 J_0)^2}\right). \tag{7}$$

This result is indeed compatible with equation (6) and by comparing these two equations the dimensionless scaling functions $a(t), b(t)$ are found to vary with foam age respectively as $J_0\eta_0$ and $1/J_0$. Remarkably, $b(t)$ extracted from creep data fully agrees with $b(t)$ obtained from oscillatory measurements (Cohen-Addad and Höhler 2004): it decreases with foam age as the inverse of the mean bubble radius (cf figure 9(b)), in agreement with the prediction of equation (4). Note that since in the scaling state there is only a single independent characteristic length scale, the Sauter mean radius R_{32} must increase in proportion to R_1.

The evolution of $a(t)$ with foam age shown in figure 9(c) indicates that coarsening also affects the timescales of viscoelastic relaxation processes. According to the mesoscopic model of creep outlined above and ignoring the high frequency contribution, $J_0\eta_0$ scales with foam age as the average time interval between coarsening induced bubble rearrangements at a given place in the foam, denoted as τ_0. This is consistent with figure 8(b) since $J_1 \ll J_0$. The relation $a(t) \propto J_0\eta_0$ obtained in the discussion following equation (7) implies that $a(t)$ must also scale with foam age as τ_0, in agreement with the data shown in figure 9(c): $a(t)$ follows asymptotically a power law, very similar to the one describing the evolution with foam age of τ_0, measured by diffusing-wave spectroscopy (Cohen-Addad and Höhler 2001).

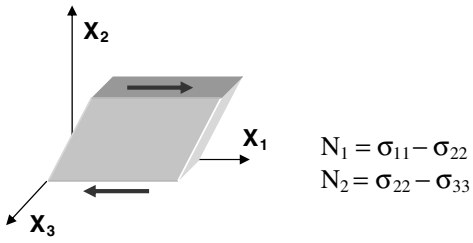

Figure 10. Definition of the first and second normal stress differences N_1 and N_2 induced by a shear σ_{12}.

3.2. Non-linear elasticity

In this section, we will discuss the rheological response of foams and concentrated emulsions in a regime of strains γ small enough to avoid yielding but large enough for deviations from linear elastic response to be significant. In isotropic elastic solids, the leading non-linear corrections to the linear shear modulus must for reasons of symmetry be of order γ^2, so corrections of the shear stress of order γ^3 are expected. A shear strain also induces stresses perpendicular to the direction of the shear, characterized by the first and second normal stress differences, denoted as N_1 and N_2 as illustrated in figure 10 (Macosko 1994). Again for reasons of symmetry, these normal stress differences are expected to be of order γ^2 and therefore represent the strongest *non-linear* elastic effect for small strains (Mal and Singh 1991). Let us point out that uniaxial strain may also lead to normal stress differences which are however to leading order a *linear* elastic effect. Recent reports of elastic normal stress differences in complex 2D flows fall into this latter category (Asipauskas *et al* 2003).

For any isotropic elastic solid whose mechanical energy is a well defined single-valued function of the instantaneous elastic strain, the shear induced first normal stress difference is intrinsically linked to the shear stress σ_{12} and shear strain γ. We will refer to this fact as the Poynting relation (Mal and Singh 1991, Poynting 1909):

$$N_1 = \sigma_{12}\gamma. \tag{8}$$

The second normal stress difference is not constrained by such a fundamental relation and depends on the physicochemical nature of the material. The first theoretical studies of non-linear elastic response in foams and emulsions concerned 2D model systems (Khan and Armstrong 1986, Princen 1983). Later, N_1 and N_2 in dry 3D ordered foams (Reinelt 1993, Reinelt and Kraynik 1993) and disordered foams (Kraynik and Reinelt 2004, Kraynik *et al* 2000) were studied. In these 3D studies, the second normal stress difference in foams and emulsions was found to be negative and in absolute value comparable to N_1, in contrast to the case for many other complex fluids such as polymers. To be able to predict the non-linear elastic response for arbitrary strains, a tensorial non-linear constitutive law is required. On the basis of a description of foam as an ensemble of film interface elements whose distribution of orientations is given by $f(\mathbf{n})$ (cf section 2.2), Doi and Otha established such a relation (Doi and Ohta 1991)[2]:

$$\boldsymbol{\sigma} = -p\mathbf{I} + T\int\int_{4\pi}(\mathbf{I} - \mathbf{n}\otimes\mathbf{n})\, f(\mathbf{n})\, \mathrm{d}\Omega, \qquad f(\mathbf{n}) = \frac{Q_0}{4\pi}\frac{[\det(\mathbf{F})]^2}{|\mathbf{F}^{\mathbf{T}}\mathbf{n}|^4}. \tag{9}$$

Q_0 is the interfacial area per unit volume in the absence of strain and $\mathbf{F}$ the deformation gradient tensor describing the applied strain (cf equation (3)) which is considered to be affine.

[2] In their paper, these authors separate the isotropic and deviatoric parts of σ, in contrast to the approach of equation (9).

The macroscopic pressure p is an average over the gas pressures in the bubbles (cf equation (2)). The integral in equation (9) must in general be evaluated numerically; only for simple shear and uniaxial strains have approximate analytical solutions been worked out. Moreover, using a pre-averaging approximation, the following analytical constitutive law has been derived on the basis of a description of foam as an ensemble of film interface elements (Larson 1997):

$$\boldsymbol{\sigma} = -p\mathbf{I} - 2G\sqrt{\mathbf{B}^{-1}}. \tag{10}$$

To make further progress we recall that the constitutive law for an incompressible isotropic material can always be cast in the following form (Mal and Singh 1991):

$$\boldsymbol{\sigma} = \beta_0\mathbf{I} + \beta_1\mathbf{B} + \beta_{-1}\mathbf{B}^{-1}. \tag{11}$$

The scalar quantities β_0, β_{-1} and β_1 are material functions depending on the invariants of the deformation tensor $\mathbf{B}$. β_0 is dominated by the average gas pressure p, but also contains a small interfacial contribution. For small strains, β_{-1} and β_1 may be approximated as constants, yielding an equation of the Mooney–Rivlin type (Macosko 1994). To determine the material functions, one has to study the dependence of the interfacial energy per foam volume W on strain induced changes of the interface element areas. For affine strain, such an expression can be established using the right Cauchy Green tensor $\mathbf{C}$ introduced in section 2.2 (Höhler *et al* 2004):

$$W(\mathbf{C}) = \frac{Ta}{V}\sum_j \sqrt{|\mathbf{C}|\mathbf{n}_j\mathbf{C}^{-1}\mathbf{n}_j}. \tag{12}$$

The sum is over all interface elements. Their unit normal vectors are denoted as $\mathbf{n}_j$ and before the strain is applied, all of them have an area denoted as a. The material functions can be obtained from $W(\mathbf{C})$ using the general formalism of continuum mechanics (Mal and Singh 1991). Recently, a simple and accurate analytical approximation of the resulting complex constitutive law has been derived (Höhler *et al* 2004):

$$W = \frac{G}{14}((\mathrm{I}_B - 3) + 6(\mathrm{II}_B - 3)) \qquad \boldsymbol{\sigma} = -p\mathbf{I} + \frac{G}{7}(\mathbf{B} - 6\mathbf{B}^{-1}). \tag{13}$$

G is the linear shear modulus and I_B and II_B are respectively the first and second invariants of $\mathbf{B}$. These equations are in good agreement with the exact theoretical results for affine simple shear and uniaxial strain up to strain of the order of a typical yield strain in foams. Moreover, equation (13) predicts $N_2/N_1 \cong -6/7$, in good agreement with quasistatic numerical simulations of sheared foams using the Surface Evolver (Kraynik and Reinelt 2004, Kraynik *et al* 2000).

4. Yielding

4.1. Experimental evidence for yielding and jamming

Many different experiments have been used to probe the passage from solid-like to liquid-like mechanical behaviour, called yielding. The maximum constant applied shear stress for which a sample will not flow defines a yield stress on the macroscopic scale (Larson 1999); the corresponding strain defines a yield strain. The yield stress can be deduced from the maximum stress in a shear start-up experiment with a constant strain rate (Khan *et al* 1988), by applying constant stresses (cf section 5.2), by studying the flow of foam on a inclined plane (Rouyer *et al* 2005) or by measuring the rheological response to an imposed oscillating stress or strain as a function of amplitude (Rouyer *et al* 2005, Saint-Jalmes and Durian 1999). This latter approach has the advantage that the maximum strain or stress and the characteristic

experimental timescale, set by the frequency, can be varied independently. Yielding appears as the passage from a predominantly elastic regime where $G' > G''$ towards predominantly viscous or plastic behaviour where $G' < G''$ (Larson 1999), observed for increasing strain or stress amplitudes. To obtain a convenient quantitative yield criterion, several authors have plotted stress amplitude as a function of strain amplitude (Mason *et al* 1996, Saint-Jalmes and Durian 1999): in the liquid-like and solid-like regimes, power laws with different exponents are observed whose intersection defines a characteristic stress. An analogous procedure based on a plot of G' versus stress amplitude gives the same value for a wet foam (Rouyer *et al* 2005), suggesting that the oscillatory yield stress obtained in such experiments is a robust quantity.

On the scale of the bubbles, yielding induced by applying macroscopic stress or strain may be defined as the onset of structural rearrangements, that modify the topology of the bubble packing and that persist if all macroscopic stress is released. Upon such rearrangements the areas of some films shrink to zero and new films are created. Viscous forces are opposed to these evolutions and thus retard the irreversible topological changes. Yielding is therefore expected to appear at strains that are an increasing function of strain rate in a shear start-up experiment. This feature has been predicted theoretically in 2D models of dry foam where viscous bulk liquid flow in the films was taken to be the dominant mechanism of dissipation (Khan and Armstrong 1987, Kraynik and Hansen 1987). Numerical results published in the latter of these papers may be described by the empirical relation:

$$\gamma_c = \gamma_{c,0} + ACa' \tag{14}$$

where γ_c is the strain where rearrangements set in and $\gamma_{c,0}$ is the value of this parameter in the quasistatic limit. $Ca' = \sqrt{3}\mu\ell(1-\phi)\dot{\gamma}/(4T)$ is a modified capillary number, μ is the liquid viscosity, ℓ the initial length of a bubble edge and A a fitted parameter. The predicted evolution of γ_c with capillary number was not detected in early shear start-up experiments (Khan *et al* 1988), due to the restricted range of strain rates explored. However, the dependence of yielding on strain rate has recently been evidenced by observing the structure in the bulk of a dry 3D foam upon shear start-up (Rouyer *et al* 2003). Shear induced rearrangements were found to occur at random positions in the probed volume, and these observations allowed one to deduce, as a function of strain and strain rate, the rearrangement probability per unit volume. The strain where this parameter rises beyond the limit of detection is identified with γ_c and represented in figure 11 as a function of strain rate. Beyond $\dot{\gamma} \cong 0.1\ \mathrm{s}^{-1}$, the increase of γ_c with strain rate indicates the presence of significant viscous forces, whereas the plateau at low strain rates strongly suggests a quasistatic regime. Let us however note that for strain rates below those shown in figure 11, coarsening induced rearrangements need to be taken into account. We have shown in section 3.1 that they lead to a slow creep or relaxation flow even for stresses and strains much too small to induce yielding. Only if the experimental timescale is sufficiently short will these phenomena be negligible and may quasistatic yielding be defined approximately. The data shown in figure 11 agree with the functional form of equation (14), but the parameter A is several orders magnitude larger than the theoretically predicted value, suggesting that viscous bulk liquid flow upon stretching of the films is not the dominant dissipation mechanism. Viscous flow in the vicinity of the Plateau borders or interfacial viscoelastic effects may play an important role in this context.

The passage from liquid-like towards solid-like behaviour, called jamming (Cipelletti and Ramos 2002, Liu and Nagel 1998), may be considered as the opposite of yielding. It can be studied by shearing the sample at slowly decreasing strain rates and measuring the stress. The extrapolation of these data to zero shear rate defines a dynamic yield stress. Such measurements are non-trivial since stress continues evolving significantly with strain rate even at very small

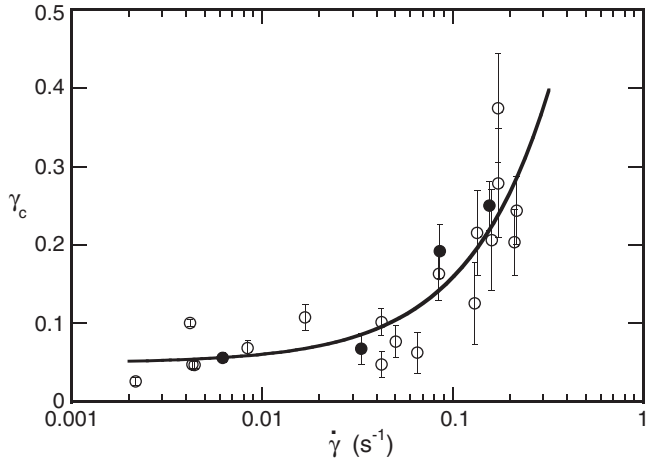

Figure 11. The strain at which shear induced rearrangements set in for a shear start-up experiment is plotted as a function of strain rate. The symbols indicate the gap width as follows: (○) 11.5 mm, (●) 16.0 mm. The gas volume fraction of the foam studied is larger than 99%. (Reprinted figure with permission from Rouyer *et al* (2003), Copyright 2003 by the American Physical Society.)

rates and also due to shear banding as explained in section 5.1. Figure 12 gives an overview of experimental yield stress data for foams and emulsions obtained using various experimental techniques over a large range of gas volume fractions. The yield stress τ_y is normalized by surface tension divided by a mean bubble radius R_1. This scaling, suggested by dimensional arguments, is widely used in the literature, despite a previous prediction that τ_y should scale as the inverse of the Sauter mean radius (Princen 1985). In all of the experiments considered, the effect of wall slip has been carefully taken into account or eliminated by roughening the surfaces in contact with the sample. The oscillatory yield stresses reported for foams and emulsions are in rough agreement and may be described by the following relation where β is a dimensionless factor close to 0.5 (cf figure 12):

$$\tau_y = \beta \frac{T}{R_1}(\phi - \phi_c)^2. \tag{15}$$

In experiments with monodispersed emulsions, the dynamic yield stress was found to agree with the oscillatory yield stress for effective dispersed volume fractions $\lesssim 0.7$ where the flow was homogeneous. However, at larger volume fractions where shear banding was observed, strong disagreement between the two types of yield stress was found (Mason *et al* 1996). The exact conditions under which heterogeneous flow develops are not yet well understood (cf section 5.1) and several authors have reported good agreement between dynamic and quasistatic yield stresses for polydispersed foams and polydispersed emulsions, even at dispersed volume fractions well beyond 0.7 (Khan *et al* 1988, Yoshimura *et al* 1987). Under oscillatory shear, heterogeneous flow has been reported to occur only at stresses clearly above the oscillatory yield stress (Rouyer *et al* 2005). Comparing experimental yield stress data with numerical simulations of totally dry random foam is non-trivial since for $\phi > 0.97$ a sharp rise of τ_y with ϕ has been reported that is not described by the empirical law of equation (15) (Gardiner *et al* 1998b). This feature may partly explain the discrepancy between the experimental data and Surface Evolver simulations of disordered dry 3D foams. Moreover, simulations using the bubble model suggest that the static yield stress strongly decreases with polydispersity (Gardiner *et al* 2000).

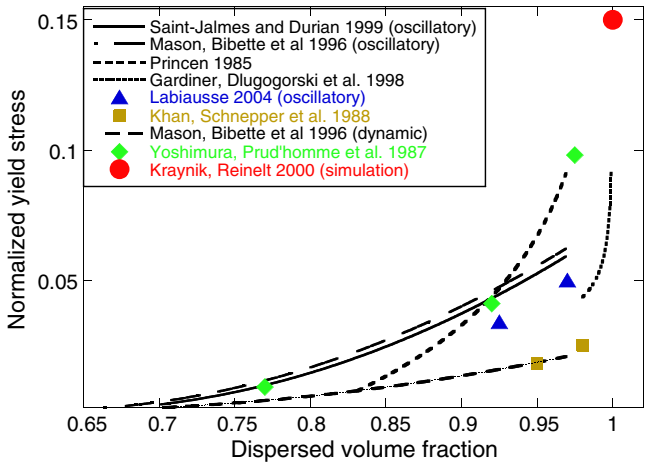

Figure 12. Yield stress data, normalized by interfacial tension divided by the mean bubble or effective droplet radius, obtained for foams and emulsions in a regime of low frequencies or shear rates, versus volume fraction of the dispersed phase. All data are experimental, except for a single point obtained by a numerical simulation. Oscillatory and dynamic yield stress data are identified in the inset. For the data reported by Princen *et al* and Yoshimura *et al*, the mean radius is R_{32}, while in all other cases it is R_1.

The complex experimental evidence shown in figure 12 suggests that parameters other than volume fraction, average radius and surface tension must have an influence on the yield stress and strain: experimental timescale, polydispersity, strain history and flow heterogeneity can be important. A recent study has shown that the impacts of these features on yield stress and elasticity are highly correlated: when normalized by the shear modulus, oscillatory shear stress data as a function of dispersed volume fraction obtained by various authors collapse onto a master curve (Rouyer *et al* 2005). Further experimental work with rigorous control of the flow field as well as well as numerical simulations may help to clarify this issue.

4.2. Memory effects

In this section, we will discuss the dependence of foam structure and rheology on strain history. Numerical simulations (Weaire *et al* 1992) as well as 2D experiments with bubble rafts covered by a glass plate (Kader and Earnshaw 1999) have shown that the topological statistics of a random foam structure are modified when it is sheared beyond the yield strain: the second central moment of the distribution of bubble coordination numbers, generally denoted as μ_2, is found to decrease with strain. These results differ from observations of bubble rafts with a free surface sheared in a Couette cell where no strain induced variation of μ_2 was observed (Dennin and Knobler 1997). Moreover, a change of bubble coordination number should modify the coarsening dynamics (Hilgenfeldt *et al* 2001b), but comparison of bubble growth in quiescent and flowing 3D foams did not reveal any such effect (Gopal and Durian 1995). Recent 3D bubble model simulations offer a possible explanation for the lack of a robust generic behaviour: the strain dependence of μ_2 is reported to depend on the strain rate and disorder as well as polydispersity (Gardiner *et al* 2000). Strain history also plays an important role in the dynamics of yielding and jamming. These features have been compared to the behaviour found for glassy materials by describing the agitation induced by flow in terms of an effective noise temperature (Liu and Nagel 1998, Sollich *et al* 1997). In this framework, the SGR model

presented in section 2.2 makes the following predictions: a system abruptly brought from high to low effective noise temperature will initially contain quenched regions of high energy that slowly relax towards a lower energy structure. The initial high energy configuration may subsequently be regenerated by applying a transient flow, a phenomenon called shear rejuvenation. Following such a flow, the rate of structural rearrangements is temporarily enhanced and then relaxes to its previous value. These rearrangements reduce temporarily the system's ability to store elastic energy and, therefore, the shear modulus should present a characteristic transient softening. Such behaviour has indeed been found experimentally for various colloidal pastes (Cloitre *et al* 2000, Derec *et al* 2003, Ozon *et al* 2003). For specific strain histories involving two distinct oscillatory shear strains, the rearrangement dynamics has been found to be accelerated at short waiting times after the shearing but slowed down at long waiting times. This phenomenon is called overageing (Viasnoff and Lequeux 2002).

The existence of shear rejuvenation and strain induced transient softening has been tested experimentally for stable foams: oscillatory measurements of the linear elastic shear modulus G' showed that after a transient flow, G' is indeed temporarily reduced and subsequently relaxes to the value obtained for quiescent foam of the same age (Höhler *et al* 1999). *In situ* diffuse transmission spectroscopy measurements showed that the mean bubble radius is not affected by the flow. The characteristic time necessary to recover the elasticity of quiescent foam was found to increase with the foam age at which the transient flow is applied, and to scale as the average time between coarsening induced bubble rearrangements measured at this age by diffusing-wave spectroscopy. This strongly suggests that the coarsening dynamics sets the timescale of the observed rheological memory effect. Furthermore, the bubble dynamics accompanying the elastic memory effect was studied by multispeckle diffusing-wave spectroscopy (Cohen-Addad and Höhler 2001). Remarkably, a transient shear flow was found to decrease the bubble rearrangement rate strongly, which is the opposite of the effect found in pastes and expected according to the analogy with glasses. In contrast to the overageing behaviour outlined above, a slowing down of the dynamics was detected in foams *directly* after the end of the transient flow. The rearrangement rate was found to relax to the value found for quiescent foams of the same age after a characteristic time denoted as T_R that increases with foam age and with the amplitude of the applied shear, as shown in figure 13. Manifestly, T_R scales linearly with foam age and strain amplitude, but it saturates above an amplitude that coincides with the crossover to liquid-like behaviour detected by macroscopic rheometry (cf figure 13(c)). This behaviour was explained by a schematic variant of the SGR model where the glassy dynamics governed by a noise temperature is replaced by a coarsening dynamics, driven by the diffusive gas exchange between neighbouring bubbles (Cohen-Addad and Höhler 2001). We conclude that foams are not soft glassy materials in the sense of the generic SGR model, but that a variant of this model taking into account the coarsening dynamics and other features specific to foams may well provide a framework for a future constitutive law, linking the bubble dynamics and macroscopic rheology. Let us finally note that both yielding and jamming have been evidenced in stress cycling experiments where strong hysteretic effects have been detected, again demonstrating the importance of strain history (DaCruz *et al* 2002, Rouyer *et al* 2003).

5. Liquid-like response

5.1. Homogeneous flow and flow induced structures

Introduction. Subjected to a steady shear stress τ beyond the yield limit τ_y, foams and concentrated emulsions present a rich variety of flow phenomena that are not yet fully

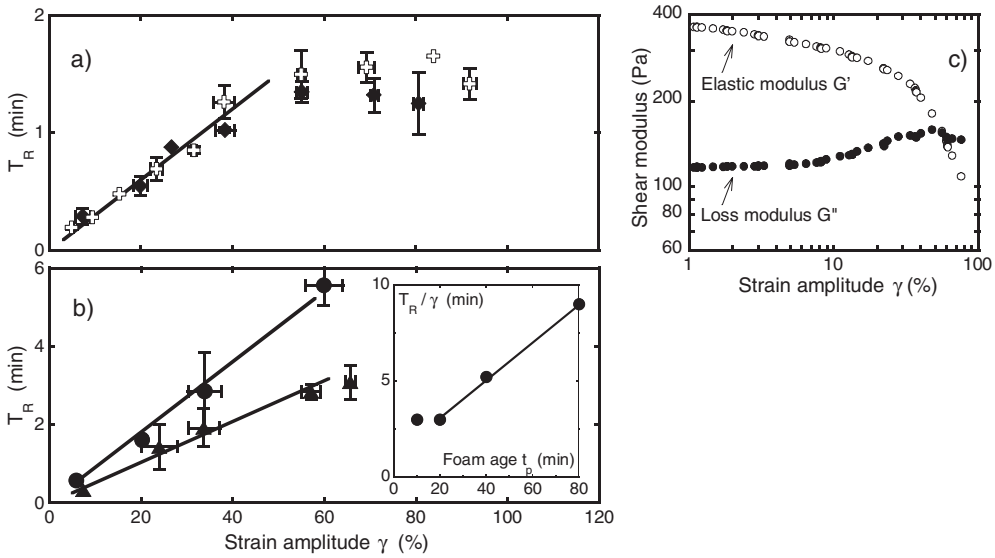

Figure 13. Time T_R necessary for rearrangement dynamics to recover after a transient oscillatory shear flow of strain amplitude γ, applied at a foam age t_p. The sample is Gillette foam with gas volume fraction 0.92. In (a), t_p is respectively equal to 10 min (diamonds) and 20 min (crosses). In (b) data with $t_p = 40$ min (triangles) and 80 min (discs) are shown. The straight lines represent linear fits. The inset in (b) shows the dependence of the corresponding slopes on foam age with a straight line indicating a linear fit for $t_p \geqslant 20$ min. (c) shows the dependence of G' and G'' on the strain amplitude for the same foam, measured at a frequency identical to that of the transient oscillatory flow. (Parts (a) and (b) reprinted with permission from Cohen-Addad and Höhler (2001), Copyright 2001 by the American Physical Society.)

understood. On a macroscopic scale, steady flow behaviour is often described by an effective viscosity η_{eff}, defined as the ratio of shear stress to the effective shear strain rate $\dot{\gamma}$, deduced from the motion of the sample boundaries. Let us note that in the presence of wall slip or if the shear rate changes across the gap, $\dot{\gamma}$ must be distinguished from the local strain rate in the foam $\dot{\gamma}_{\text{local}}$, defined at a length scale smaller than the sample size but much larger than the bubbles (cf section 2.2). Experiments on 3D foams and emulsions (Gopal and Durian 1999, Khan *et al* 1988, Mason *et al* 1996, Princen and Kiss 1989) show that over a large range of shear rates η_{eff} is many orders of magnitude larger than the viscosity of the continuous phase. This is a consequence of the yield stress, whose origin at the bubble scale was discussed in section 2.2. The measured flow curves $\tau(\dot{\gamma})$ are often fitted using the phenomenological Herschel–Bulkley law (Larson 1999) where ξ and n are empirical parameters:

$$\begin{aligned} &\dot{\gamma} = 0 \qquad \text{for } \tau < \tau_y \\ &\tau = \tau_y + \xi \dot{\gamma}^n \qquad \text{for } \tau \geqslant \tau_y. \end{aligned} \tag{16}$$

Note that for $n = 1$, this expression reduces to the Bingham law. A relationship of the form of equation (16) with $n = 2/3$ has been predicted theoretically, on the basis of an analysis of viscous dissipation in the neighbourhood of the Plateau borders (Schwartz and Princen 1987). Flow behaviour that may be described by equation (16) is also predicted by the SGR model (Sollich 1998) (cf section 2.2) as well as by 2D and 3D numerical bubble model simulations (Durian 1995, Gardiner *et al* 2000). Several authors have fitted experimental data for foams and emulsions over a wide range of effective shear rates using the Herschel–Bulkley law with n ranging from 0.25 to 1 (Denkov *et al* 2005, Gopal and Durian 1999, Khan *et al* 1988,

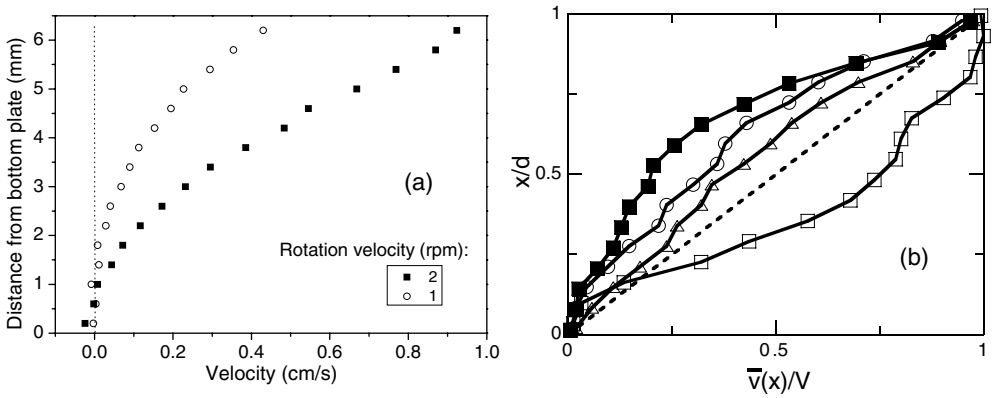

Figure 14. (a) Velocity profile in a polydisperse emulsion, flowing in the gap of a cone plate rheometer (figure reprinted with permission from Coussot *et al* (2002b), Copyright 2002 by the American Physical Society). (b) Normalized velocity profile of foam undergoing steady shear flow in a sliding plate rheometer. d is the gap width and V the velocity of the mobile plate with respect to the fixed plate. The symbols correspond to experiments made with nominally identical samples for different values of d and V. The fluctuations of the profile were found to be statistical and do not present any systematic variations with d and V in the range explored. The dashed straight line represents the velocity profile expected for a uniform strain rate. At the beginning of the shear start-up flow the normalized velocity data remain close to this line. (Figure modified with permission from Rouyer *et al* (2003), Copyright 2003 by the American Physical Society.)

Princen and Kiss 1989). However, flow behaviour can be more complex, as first pointed out by Mason *et al* (1996). In the following, we present several recent rheological experiments on 3D foams and emulsions showing that the Herschel–Bulkley law does not capture all of the physics that governs the flow of these materials: at low strain rates, liquid-like and solid-like regions can coexist in the same sample, even under homogeneous stress. Many recent theoretical publications propose interpretations of such heterogeneous flow or shear banding in complex fluids in terms of flow curves where stress does not increase monotonically with local strain rate, as discussed in a recent review (Ajdari 2002).

Flow under homogeneous stress. Few direct observations of the local velocity field in foams or concentrated emulsions flowing under *homogeneous* applied shear stress have been published: a MRI study of an emulsion, steadily sheared in a cone and plate geometry, has shown coexisting liquid-like and solid-like regions (Coussot *et al* 2002b). These data, shown in figure 14(a), indicate that the width of the solid-like region decreases with increasing cone rotation velocity and thus with effective strain rate, so homogeneous flow may occur for sufficiently high strain rates. Moreover, the velocity field of bubbles in the bulk of a dry 3D foam upon shear start-up in a sliding plate geometry was observed by an optical imaging technique (Rouyer *et al* 2003). The macroscopic deformation remained to a good approximation homogeneous up to strains typically one order of magnitude larger than the yield strain, because bubble rearrangements were localized and randomly distributed throughout the gap. At larger strains, the bubble velocity profile became non-linear and fluctuating as illustrated in figure 14(b), which can be interpreted as the onset of shear banding. Evidence for heterogeneous flow under simple shear was also found in quasistatic Surface Evolver simulations of ordered dry 3D foam (Reinelt and Kraynik 2000) and disordered dry 2D foam (Kabla and Debregeas 2003), but not in simulations of disordered foams using the bubble model (Durian 1995, 1997, Gardiner *et al* 2000).

Flow under heterogeneous stress. Several experimental studies of foam flow have been performed using the cylindrical Couette geometry, in which shear stress varies under stationary conditions as $\tau_{r\theta}(r) \propto 1/r^2$ where r is the distance from the axis of symmetry (Macosko 1994). For a complex fluid with yield stress τ_y and a shear rate low enough for viscous forces to be small, this implies that the local strain rate must be zero in the sample except in a region close to the inner cylinder. Note that such behaviour induced by stress *heterogeneity* must be distinguished from shear banding that appears spontaneously under *homogeneous* shear stress (as in figure 14).

We will now discuss experimental data obtained with a 3D cylindrical Couette geometry. The velocity field in monodispersed emulsions upon shear start-up has been visualized by painting a black stripe on the free sample surface (Mason *et al* 1996). For volume fractions $\phi > 0.7$, the formation of a sharply localized shear band was observed. It does not appear to result from stress heterogeneity since it was randomly located in the gap. Remarkably, the flow for volume fractions $\phi < 0.7$ was found to be homogeneous in these experiments, suggesting that shear banding may not be a universal feature of any flowing emulsion. The velocity profiles in steadily flowing emulsions and foams with $\phi > 0.7$ have been studied by MRI (Bertola *et al* 2003, Coussot *et al* 2002b, Rodts *et al* 2005) and by dynamic light scattering (Becu *et al* 2005, Salmon *et al* 2003). These data differ from those reported for shear start-up in that no *sharply localized* shear band is observed, in qualitative agreement with a multiple light scattering study of 3D foam of gas volume fraction 0.92 that steadily flows in a Couette geometry (Gopal and Durian 1999). The following constitutive equation was found to describe the relation between stress and the *local* strain rate in an emulsion and a foam steadily sheared in a wide gap Couette geometry (Coussot *et al* 2002b, Rodts *et al* 2005):

$$\begin{aligned} &\dot{\gamma}_{\text{local}} = 0 \qquad \text{for } \tau < \tau_c \\ &\tau = \tau_c(\dot{\gamma}_{\text{local}}/\dot{\gamma}_c)^m \qquad \text{for } \tau \geqslant \tau_c. \end{aligned} \tag{17}$$

The fitted parameter m was in the range 0.2–0.3. τ_c is a critical stress, existing at the interface between flowing and solid-like regions, and $\dot{\gamma}_c$ is a critical local shear rate below which steady flow is reported to be impossible. For $\dot{\gamma}_{\text{local}} \geqslant \dot{\gamma}_c$, power law fluid behaviour is predicted throughout the sample. If $\dot{\gamma} < \dot{\gamma}_c$, the effective macroscopic behaviour is controlled by a balance of coexisting liquid-like and solid-like phases. The cited MRI data present a discontinuous jump of $\dot{\gamma}_{\text{local}}$ as a function of the radial coordinate, at the boundary between flowing and solid-like regions, in agreement with equation (17) but in contradiction with the Herschel–Bulkley law. Further evidence has been obtained using dynamic light scattering measurements of the velocity field in a monodispersed emulsion, steadily sheared in a Couette cell (Salmon *et al* 2003). These data could only be fitted to equation (17) if the model parameters were allowed to depend on stress.

Several flow velocity field measurements have been carried out in the 2D cylindrical Couette geometry. The samples were either bubble monolayers confined between the glass plates of a Hele–Shaw cell (Debregeas *et al* 2001) or bubble rafts floating on a liquid (Lauridsen *et al* 2002). In the limit of very slow steady shear where viscous interactions may be expected to be insignificant, the flow behaviours observed in these two experiments differ: in the Hele–Shaw cell experiment, the average tangential bubble velocity was found to drop exponentially to zero with distance from the inner sample boundary, on the scale of a few bubble diameters (Debregeas *et al* 2001), whereas bubble motion throughout the bulk of the system was reported in bubble raft shear experiments (Lauridsen *et al* 2002). Moreover, the macroscopic flow curve obtained in the latter measurements over a wide range of strain rates could be fitted approximately by the Herschel–Bulkley model with exponent 1/3 (Pratt and Dennin 2003). Recently, a discontinuous variation of strain rate with radius at the interface between flowing

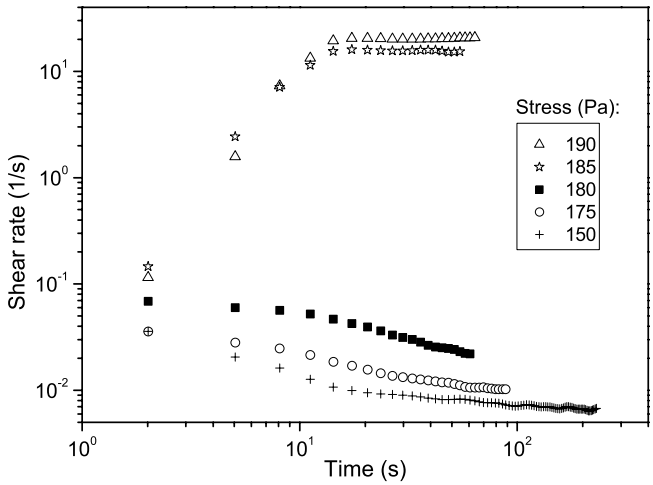

Figure 15. Effective shear rate versus time, obtained for foam (Gillette shaving cream) subjected to a step stress. Note that an increase of the imposed stress of less than 3% changes the shear rate at long times by several orders of magnitude. (Figure reprinted with permission from DaCruz *et al* (2002), Copyright 2002 by the American Physical Society.)

and solid-like regions of the bubble raft has been detected in such experiments at very low effective shear rates, in qualitative agreement with equation (17) (Lauridsen *et al* 2004). Other recent studies of dissipation in flowing 2D foam concern the viscous drag on a cylindrical obstacle (Dollet *et al* 2005) or flow through a constriction (Asipauskas *et al* 2003).

More experimental and theoretical work is needed to understand quantitatively all aspects of the steady flow of foams and emulsions. Realistic descriptions of viscous and elastic bubble interactions, shear flow induced bubble segregation according to size (Herzhaft 2002, Quilliet *et al* 2005), dilatancy (defined in this context as the migration of the liquid content driven by heterogeneous stress) (Marze *et al* 2005, Rioual *et al* 2005, Weaire and Hutzler 2003) and shear induced bubble rupture (Mason and Rai 2003) may have to be considered.

5.2. Thixotropy and viscosity bifurcation

Figure 15 shows the time evolution of the effective strain rate in foam subjected to a step shear stress of amplitude τ. Such flow induced time evolution of the effective viscosity is called thixotropy (Macosko 1994). Note that the experimental timescale of these experiments is sufficiently short for the ageing processes presented in section 2.1 to be negligible. For $\tau < \tau_y$, the strain rate progressively decreases, whereas for $\tau > \tau_y$, it increases and converges to a steady state value. Remarkably, the effective viscosity at long times varies discontinuously as a function of the applied constant stress τ at $\tau = \tau_y$: this behaviour, called viscosity bifurcation (DaCruz *et al* 2002), is incompatible with the Herschel–Bulkley law which predicts a continuous divergence of the effective viscosity as a function of τ in the vicinity of $\tau = \tau_y$. The bifurcation under steady state conditions is described at least qualitatively by equation (17).

5.3. Flow dynamics on the bubble scale

Steady flow of 3D foams. The steady flow dynamics of 3D foam on the bubble scale has been studied experimentally in samples with 0.92 gas volume fraction, using diffusing-wave

spectroscopy, a non-invasive multiple light scattering technique (Earnshaw and Wilson 1995, Gopal and Durian 1995, 1999). These data did not provide any evidence for marked strain localization effects. As a function of strain rate $\dot{\gamma}$, yield strain γ_y and typical duration of a rearrangement τ_d, three regimes of different local dynamics have been identified and explained at least schematically (Gopal and Durian 1999): for $\dot{\gamma}$ well above γ_y/τ_d, the DWS data indicate a continuous flow with a convective laminar profile. Indeed, under these conditions new rearrangements are expected to be triggered before the preceding ones are finished. For strain rates well below γ_y/τ_d, macroscopic flow is accomplished by intermittent rearrangements of small bubble clusters, occurring at a rate $\dot{\gamma}/\gamma_y$. This is consistent with a schematic model where the local strain continuously builds up at a rate $\dot{\gamma}$ and is reset to zero whenever it reaches γ_y. At very low strain rates, the rate of coarsening induced rearrangements at a given place in the sample, denoted as $1/\tau_0$, exceeds that of strain induced rearrangements. A crossover to this latter regime is expected and observed for $\dot{\gamma} = \gamma_y/\tau_0$. Remarkably, the reported dependence of the effective viscosity on $\dot{\gamma}$ does not present any marked features at the crossover between the different regimes discussed here (Gopal and Durian 1999). Numerical simulation studies of bubble dynamics in flowing 3D foams have been carried out so far only for dry ordered structures in the quasistatic regime, using the Surface Evolver software. Rearrangements forming complex cascades were found to occur throughout the sample (Reinelt and Kraynik 2000).

Steady flow of 2D foams. Insight into the local dynamics in flowing 2D foams has been obtained by experiments and numerical studies. The bubble model predicts the existence of a well defined quasistatic shear flow regime where stress as well as number of rearrangements per bubble and unit strain are independent of strain rate (Durian 1995, Tewari *et al* 1999), in agreement with vertex model simulations (Okuzono and Kawasaki 1995), and observations of bubble rafts sheared in a Couette geometry (Dennin and Knobler 1997, Pratt and Dennin 2003), but in contrast with a simulation using the Potts model (Jiang *et al* 1999). The event size, defined as the number of bubbles participating in a rearrangement, has been reported to be typically of the order of a few bubbles for dry foams (cf figure 16) but to increase on average with the liquid volume fraction (Hutzler *et al* 1995, Tewari *et al* 1999). Moreover, experimental studies of sheared bubble rafts have shown that the distribution of stress drops upon events follow a power law with a cut-off (Lauridsen *et al* 2002). Such a law also describes the distribution of elastic energy drops in bubble model simulations where the cut-off at large energies was found to be independent of the system size for large dry systems (Durian 1997). These consistent experimental and simulation results are in contrast to previous vertex model simulations of dry foam where the energy drop distribution was reported to be limited by the system size, suggesting self-organized critical behaviour (Okuzono and Kawasaki 1995). However, in the wet limit, recent bubble model simulations have evidenced large, possibly system-wide events (Tewari *et al* 1999). Another recently investigated feature of steadily sheared foams is bubble velocity fluctuations. Studies using the bubble model have shown a crossover from Gaussian fluctuations for $\dot{\gamma} \gg \gamma_y/\tau_d$ towards strong non-Gaussian fluctuations governed by bubble rearrangement dynamics for $\dot{\gamma} \ll \gamma_y/\tau_d$ (Ono *et al* 2003). Experimental studies of sheared bubble rafts have shown that velocity fluctuations vary with position across the discontinuity in rate of strain mentioned in section 5.1 (Dennin 2005). Moreover, there is strong evidence that an effective temperature may be a useful measure of velocity fluctuations in this context (Langer and Liu 2000, Ono *et al* 2002). Several recent 2D studies have focused on bubble dynamics in localized quasistatic flows (Cox *et al* 2004, Debregeas *et al* 2001, Kabla and Debregeas 2003): in the heterogeneous stress field of a cylindrical Couette device, strong fluctuations involving roll-like bubble motion were identified. Simple shear as well as

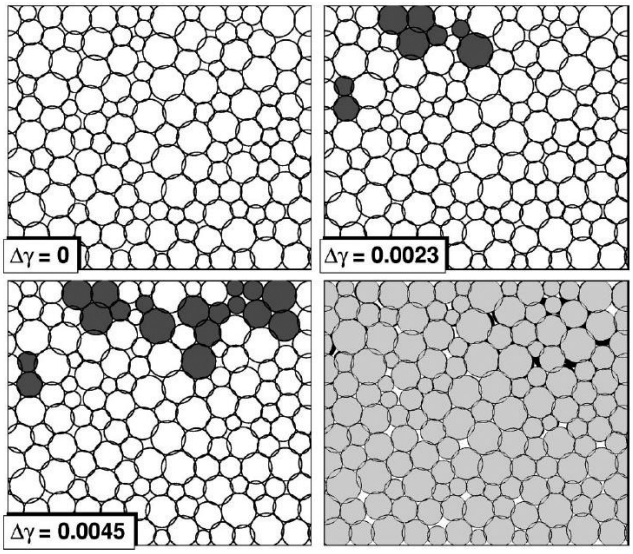

Figure 16. Sequence of snapshots illustrating the nature and time evolution of a typical shear induced bubble rearrangement in dry 2D foam, simulated using the bubble model. Bubbles that change overlapping neighbours as the applied shear $\Delta\gamma$ increases are marked in grey. The fourth frame shows the final configuration with bubbles in light grey superimposed on the initial configuration with bubbles in black. (Figure reprinted with permission from Tewari *et al* (1999), Copyright 1999 by the American Physical Society.)

cylindrical Couette Surface Evolver simulations evidenced spatial stress fluctuations related to the formation of shear bands close to the sample boundary.

Some recent work focuses on 2D foam rheology beyond the quasistatic regime: a viscous froth model has been developed in the framework of Surface Evolver simulations for describing flow in Hele–Shaw cells where the viscous drag of the lamellae on the walls is taken into account (Cox *et al* 2004, Kern *et al* 2004, Cox 2005). It has been applied to the study of microfluidic devices, on the basis of ordered 2D foam flowing in channel geometries (Drenckhan *et al* 2005).

6. Conclusion and outlook

The work outlined in this review shows that liquid foam rheology is governed by processes and properties on a large range of length scales. The rheology of the gas–liquid interfaces, governed by processes on the molecular scale, as well as mesoscopic bubble rearrangements have been shown to be of crucial importance for the macroscopic response. This interplay goes beyond the models developed in pioneering studies of foam rheology, explaining the elastic response in terms of average bubble radius, surface tension and gas volume fraction. The experimental evidence shows that the slow linear viscoelastic relaxations of foams strongly differ from those of glassy materials. However, the question remains of whether soft glassy rheology models nevertheless capture the physics of foam jamming and yielding. Moreover, it is not clear under what conditions foam flow is intrinsically heterogeneous. The vanishing of static elasticity at increasing liquid fractions also raises open fundamental questions. Its experimental study is difficult due to the strong drainage in very wet foams and may require microgravity conditions. The coupling between rheology, drainage and coalescence is in itself

an interesting and insufficiently explored topic. Further experiments and numerical studies probing how local foam structure and dynamics are linked to the macroscopic rheological behaviour will help to make progress towards a full theoretical understanding of liquid foam rheology.

Acknowledgments

We would like to acknowledge stimulating discussions with M Cates, P Coussot, D Durian, F Graner, A Kraynik, E Lorenceau, F Rouyer, P Sollich and D Weaire. We also thank Y Yip and S Vincent-Bonnieu for providing figures 2(b) and 3.

References

Abd el Kader A and Earnshaw J C 1999 *Phys. Rev. Lett.* **82** 2610–3
Adamson A 1990 *Physical Chemistry of Surfaces* (New York: Wiley)
Ajdari A 2002 *Slow Relaxations and Nonequilibrium Dynamics in Condensed Matter* vol LXXVII, ed J L Barrat, J Kurchan and J Dalibard (Berlin: Springer) pp 43–71
Asipauskas M, Aubouy M, Glazier J A, Graner F and Jiang Y 2003 *Granular Matter* **5** 71–4
Aubouy M, Jiang Y, Glazier J A and Graner F 2003 *Granular Matter* **5** 67–70
Bachelor G K 1970 *J. Fluid Mech.* **41** 545–70
Barrat J-L, Feigelman M, Kurchan J and Dalibard J (ed) 2003 *Slow Relaxations and Nonequilibrium Dynamics in Condensed Matter* (Berlin: Springer)
Becu L, Grondin P, Colin A and Manneville S 2005 *Colloids Surf.* A **263** 146–52
Bertola V, Bertrand F, Tabuteau H, Bonn D and Coussot P 2003 *J. Rheol.* **47** 1211–26
Bhakta A and Ruckenstein E 1997 *J. Colloid Interface Sci.* **191** 184–201
Bolton F and Weaire D 1990 *Phys. Rev. Lett.* **65** 3449–51
Bouchaud J P 1992 *J. Physique* I **2** 1705
Brakke K 1992 *Exp. Math.* **1** 141
Bretherton F P 1961 *J. Fluid Mech.* **10** 166–88
Buzza D M A, Lu C-Y D and Cates M E 1995 *J. Physique* II **5** 37–52
Calvert J R 1990 *Int. J. Heat Fluid Flow* **11** 236–41
Cantat I, Kern N and Delannay R 2004 *Europhys. Lett.* **65** 726–32
Carrier V and Colin A 2003 *Langmuir* **19** 4535–8
Cates M E 2002 *Slow Relaxations and Nonequilibrium Dynamics in Condensed Matter* vol LXXVII, ed J L Barrat, J Kurchan and J Dalibard (Berlin: Springer) pp 74–130
Cipelletti L and Ramos L 2002 *Curr. Opin. Colloid Interface Sci.* **7** 228–34
Cloitre M, Borrega R and Leibler L 2000 *Phys. Rev. Lett.* **85** 4819–22
Cohen-Addad S, Hoballah H and Höhler R 1998 *Phys. Rev.* E **57** 6897–901
Cohen-Addad S and Höhler R 2001 *Phys. Rev. Lett.* **86** 4700–3
Cohen-Addad S and Höhler R 2004 unpublished
Cohen-Addad S, Höhler R and Khidas Y 2004 *Phys. Rev. Lett.* **93** 028302
Coussot P, Nguyen Q D, Huynh H T and Bonn D 2002a *Phys. Rev. Lett.* **88** 175501
Coussot P, Raynaud J S, Bertrand F, Moucheront P, Guilbaud J P, Huynh H T, Jarny S and Lesueur D 2002b *Phys. Rev. Lett.* **88** 218301–4
Cox S 2005 *Colloids Surf.* A **263** 81–9
Cox S, Weaire D and Glazier J A 2004 *Rheol. Acta* **43** 442–8
DaCruz F, Chevoir F, Bonn D and Coussot P 2002 *Phys. Rev.* E **66** 051305
Debregeas G, Tabuteau H and Di Meglio J-M 2001 *Phys. Rev. Lett.* **87** 178305
Denkov N D, Subramanian V, Gurovich D and Lips A 2005 *Colloids Surf.* A **263** 129–45
Dennin M 2005 *Colloids Surf.* A **263** 76–80
Dennin M and Knobler C M 1997 *Phys. Rev. Lett.* **78** 2485–8
Derec C, Ajdari A and Lequeux F 2001 *Eur. Phys. J.* E **4** 355–61
Derec C, Ducouret G, Ajdari A and Lequeux F 2003 *Phys. Rev.* E **67** 061403
Derjaguin B V 1933 *Kolloid Z.* **64** 1–6
Djabbarah N F and Wasan D T 1982 *Chem. Eng. Sci.* **37** 175–84

Doi M and Ohta T 1991 *J. Chem. Phys.* **95** 1242–8
Dollet B, Elias F, Quilliet C, Huillier A, Aubouy M and Graner F 2005 *Colloids Surf.* A **263** 101–10
Drenckhan W, Cox S J, Delaney G, Holste H, Weaire D and Kern N 2005 *Colloids Surf.* A **263** 52–64
Durand M and Langevin D 2002 *Eur. Phys. J.* E **7** 35–44
Durian D J 1995 *Phys. Rev. Lett.* **75** 4780–3
Durian D J 1997 *Phys. Rev.* E **55** 1739–51
Durian D J, Weitz D A and Pine D J 1991 *Phys. Rev.* A **44** R7902–5
Earnshaw J C and Wilson M 1995 *J. Phys.: Condens. Matter* **7** L49–53
Edwards D, Brenner H and Wasan D 1991 *Interfacial Transport Processes and Rheology* (London: Butterworth-Heinemann)
Enzendorfer C, Harris R A, Valko P, Economides M J, Fokker P A and Davies D D 1995 *J. Rheol.* **39** 345–58
Ferry J 1980 *Viscoelastic Properties of Polymers* (New York: Wiley)
Fortes M A, Teixeira P I C and Vaz M F 2002 *Phys. Rev. Lett.* **89** 278302
Gardiner B S, Dlugogorski B Z and Jameson G J 1998a *Fire Safety J.* **31** 61–75
Gardiner B S, Dlugogorski B Z and Jameson G J 2000 *J. Non-Newton. Fluid Mech.* **92** 151–66
Gardiner B S, Dlugogorski B Z, Jameson G J and Chhabra R P 1998b *J. Rheol.* **42** 1437–50
Glazier J A, Anderson M P and Grest G S 1990 *Phil. Mag.* B **62** 614–45
Glazier J A and Weaire D 1992 *J. Phys.: Condens. Matter* **4** 1867–94
Gopal A D and Durian D J 1995 *Phys. Rev. Lett.* **75** 2610–3
Gopal A D and Durian D J 1999 *J. Colloid Interface Sci.* **213** 169–78
Gopal A D and Durian D J 2003 *Phys. Rev. Lett.* **91** 188303
Grest G S, Anderson M P and Srolovitz D J 1988 *Phys. Rev.* B **38** 4752–60
Hébraud P and Lequeux F 1998 *Phys. Rev. Lett.* **81** 2934–7
Hébraud P, Lequeux F and Palierne J-F 2000 *Langmuir* **16** 8296–9
Hemar Y, Hocquart R and Lequeux F 1995 *J. Physique* II **5** 1567–76
Herzhaft B 2002 *J. Colloid Interface Sci.* **247** 412–23
Herzhaft B, Kakadjian S and Moan M 2005 *Colloids Surf.* A **263** 153–64
Hilgenfeldt S, Koehler S A and Stone H A 2001a *Phys. Rev. Lett.* **86** 4704–7
Hilgenfeldt S, Kraynik A M, Koehler S A and Stone H A 2001b *Phys. Rev. Lett.* **86** 2685–8
Hoballah H, Höhler R and Cohen-Addad S 1997 *J. Physique* II **7** 1215–24
Höhler R, Cohen-Addad S and Asnacios A 1999 *Europhys. Lett.* **48** 93–8
Höhler R, Cohen-Addad S and Hoballah H 1997 *Phys. Rev. Lett.* **79** 1154–7
Höhler R, Cohen-Addad S and Labiausse V 2004 *J. Rheol.* **48** 679–90
Hutzler S and Weaire D 2000 *Phil. Mag. Lett.* **80** 419–25
Hutzler S, Weaire D and Bolton F 1995 *Phil. Mag.* B **71** 277–89
Jiang Y, Swart P J, Saxena A, Asipauskas M and Glazier J A 1999 *Phys. Rev.* E **59** 5819–32
Kabla A and Debregeas G 2003 *Phys. Rev. Lett.* **90** 258303
Kern N and Weaire D 2003 *Phil. Mag.* **83** 2973–87
Kern N, Weaire D, Martin A, Hutzler S and Cox S J 2004 *Phys. Rev.* E **70** 041411
Khan S A and Armstrong R C 1986 *J. Non-Newton. Fluid Mech.* **22** 1–22
Khan S A and Armstrong R C 1987 *J. Non-Newton. Fluid Mech.* **25** 61–92
Khan S A and Prud'homme R 1996 *Foams* (New York: Dekker)
Khan S A, Schnepper C A and Armstrong R C 1988 *J. Rheol.* **32** 69–92
Koehler S A, Hilgenfeldt S and Stone H A 2000 *Langmuir* **16** 6327–41
Kraynik A M and Hansen M G 1987 *J. Rheol.* **31** 175–205
Kraynik A M and Reinelt D A 1996 *J. Colloid Interface Sci.* **181** 511–20
Kraynik A M and Reinelt D A 2004 *14th Int. Cong. on Rheology (Seoul, Korea)*
Kraynik A M, Reinelt D A and van Swol F 2003 *Phys. Rev.* E **67** 031403–11
Kraynik A M, Reinelt D A and van Swol F 2000 *3rd Euro Conf. on Foams, Emulsions and Applications* pp 191–8
Kraynik A M, Reinelt D A and van Swol F 2004 *Phys. Rev. Lett.* **93** 208301
Labiausse V 2004 *PhD Thesis* Université de Marne-la-Vallée
Lacasse M D, Grest G S, Levine D, Mason T G and Weitz D A 1996 *Phys. Rev. Lett.* **76** 3448–51
Langer S A and Liu A J 1997 *J. Phys. Chem.* B **101** 8667–71
Langer S A and Liu A J 2000 *Europhys. Lett.* **49** 68
Langevin D 2000 *Adv. Colloid Interface Sci.* **88** 209–22
Larson R G 1997 *J. Rheol.* **41** 365–72
Larson R G 1999 *The Structure and Rheology of Complex Fluids* (New York: Oxford University Press)
Lauridsen J, Chanan G and Dennin M 2004 *Phys. Rev. Lett.* **93** 018303

Lauridsen J, Twardos M and Dennin M 2002 *Phys. Rev. Lett.* **89** 098303
Levich V G 1962 *Physical Hydrodynamics* (Englewood Cliffs, NJ: Prentice-Hall)
Liu A and Nagel S 1998 *Nature* **396** 21
Liu A J, Ramaswamy S, Mason T G, Gang H and Weitz D A 1996 *Phys. Rev. Lett.* **76** 3017–20
Macosko C 1994 *Rheology, Principles, Measurements and Applications* (New York: Wiley–VCH)
Mal A and Singh S 1991 *Deformation of Elastic Solids* (London: Prentice-Hall)
Marze S P L, Saint-Jalmes A and Langevin D 2005 *Colloids Surf.* A **263** 121–8
Mason T G, Bibette J and Weitz D A 1995 *Phys. Rev. Lett.* **75** 2051–4
Mason T G, Bibette J and Weitz D A 1996 *J. Colloid Interface Sci.* **179** 439–48
Mason T G and Rai P K 2003 *J. Rheol.* **47** 513–33
Morse D C and Witten T A 1993 *Europhys. Lett.* **22** 549–55
Müller W and Di Meglio J M 1999 *J. Phys.: Condens. Matter* **11** L209–15
Mullins W W 1986 *J. Appl. Phys.* **59** 1341–9
Neethling S J, Lee H T and Cilliers J J 2002 *J. Phys.: Condens. Matter* **14** 331–42
Okuzono T and Kawasaki K 1995 *Phys. Rev.* E **51** 1246–53
Okuzono T, Kawasaki K and Nagai T 1993 *J. Rheol.* **37** 571–86
Ono I K, O'Hern C S, Durian D J, Langer S A, Liu A J and Nagel S R 2002 *Phys. Rev. Lett.* **89** 095703
Ono I K, Tewari S, Langer S A and Liu A J 2003 *Phys. Rev.* E **67** 061503
Ozon F, Narita T, Knaebel A, Debregeas G, Hebraud P and Munch J-P 2003 *Phys. Rev.* E **68** 032401
Picard G, Ajdari A, Bocquet L and Lequeux F 2002 *Phys. Rev.* E **66** 051501
Poynting J H 1909 *Proc. R. Soc.* A **82** 546–9
Pratt E and Dennin M 2003 *Phys. Rev.* E **67** 051402
Princen H M 1983 *J. Colloid Interface Sci.* **91** 160–75
Princen H M 1985 *J. Colloid Interface Sci.* **105** 150–71
Princen H M and Kiss A D 1986 *J. Colloid Interface Sci.* **112** 427–37
Princen H M and Kiss A D 1989 *J. Colloid Interface Sci.* **128** 176–85
Princen H M and Mason S G 1965 *J. Colloid Sci.* **20** 353–75
Quilliet C, Idiart M A P, Dollet B, Berthier L and Yekini A 2005 *Colloids Surf.* A **263** 95–100
Reinelt D A 1993 *J. Rheol.* **37** 1117–39
Reinelt D A and Kraynik A M 1993 *J. Colloid Interface Sci.* **159** 460–70
Reinelt D A and Kraynik A M 2000 *J. Rheol.* **44** 453–71
Rioual F, Hutzler S and Weaire D 2005 *Colloids Surf.* A **263** 117–20
Rodts S, Baudez J C and Coussot P 2005 *Europhys. Lett.* **69** 636–42
Rouyer F, Cohen-Addad S and Hohler R 2005 *Colloids Surf.* A **263** 111–6
Rouyer F, Cohen-Addad S, Vignes-Adler M and Höhler R 2003 *Phys. Rev.* E **67** 021405
Saint-Jalmes A and Durian D J 1999 *J. Rheol.* **43** 1411–22
Saint-Jalmes A and Langevin D 2002 *J. Phys.: Condens. Matter* **14** 9397–412
Saint-Jalmes A, Vera M U and Durian D J 2000 *Eur. Lett.* **50** 695–701
Salmon J-B, Bécu L, Manneville S and Colin A 2003 *Eur. Phys. J.* E **10** 209–21
Schwartz L W and Princen H M 1987 *J. Colloid Interface Sci.* **118** 201–11
Sollich P 1998 *Phys. Rev.* E **58** 738–59
Sollich P, Lequeux F, Hébraud P and Cates M E 1997 *Phys. Rev. Lett.* **78** 2020–23
Stamenovic D 1991 *J. Colloid Interface Sci.* **145** 255–9
Tewari S, Schiemann D, Durian D J, Knobler C M, Langer S A and Liu A J 1999 *Phys. Rev.* E **60** 4385–96
Vandewalle N and Lentz J F 2001 *Phys. Rev.* E **64** 021507
Vera M U and Durian D J 2002 *Phys. Rev. Lett.* **88** 088304
Verbist G, Weaire D and Kraynik A M 1996 *J. Phys.: Condens. Matter* **8** 3715–31
Viasnoff V and Lequeux F 2002 *Phys. Rev. Lett.* **89** 065701
Weaire D, Bolton F, Herdtle T and Aref H 1992 *Phil. Mag. Lett.* **66** 293
Weaire D and Fortes M A 1994 *Adv. Phys.* **43** 685–738
Weaire D and Hutzler S 1999 *The Physics of Foams* (Oxford: Oxford University Press)
Weaire D and Hutzler S 2003 *Phil. Mag.* **83** 2747–60
Weaire D and Kermode J P 1984 *Phil. Mag.* B **50** 379–95
Weaire D and Phelan R 1996 *J. Phys.: Condens. Matter* **8** L37–43
Yoshimura A S, Prud'homme R K, Princen H M and Kiss A D 1987 *J. Rheol.* **31** 699–710